Optimization of spheroid formation: the case of Mn9D cells as a novel tool to assess cytotoxicity and neurodegeneration

Major Qualifying Project completed at the University of Nova Gorica, Slovenia submitted by:

Britney Atwater

Lauren DiFelice

Andrea DiGioia

Amanda Ippolito

December 17, 2013

Keywords:
Spheroids
Pesticides
Neurodegeneration
In vitro

Advisor:
Professor Marsha Rolle

Table of Contents

Table of Figures

Table of Tables

Authorship

Each member contributed equally to the writing and editing of this report.

Acknowledgements

We would like to extend our sincerest gratitude to our primary advisor, Professor Marsha Rolle for her guidance and support throughout our project. We would also like to thank Professor Elsa Fabbretti, Professor Giulietta Pinato, and Professor Tanja Dominko for generously donating their time to sponsor our project. Additionally, we are grateful for the day to day help from Tanja Bele, Marko Snajder, and the staff at the University of Nova Gorica.

Abstract

While many published reports link pesticide exposure to the development of neurological disorders, such as Parkinson's disease, the mechanisms through which the neurodegeneration occurs are not fully understood. Furthermore, researchers have difficulties predicting the toxic effects of pesticides on humans because traditional two dimensional cell culture does not provide physiologically relevant data. As a result, we aimed to design a repeatable, user friendly, and scalable process utilizing three dimensional cell culture of Mn9D cells as an *in vitro* model to study the cytotoxicity and neurodegeneration caused by chronic pesticide exposure. Mn9D cells were used because they are well-established as a model for studying neurodegeneration. Additionally, there have not been any published studies that utilize Mn9D cells in three dimensional cell culture. We saw this as an opportunity to develop a new approach to form three dimensional microtissues, called spheroids, that model cell-to-cell interactions of neurons which could be used as a screening tool for testing the toxicity levels of pesticides. To design an inexpensive and efficient process, we tested various combinations of cell suspension platforms and spheroid characteristics to determine the optimal spheroid for toxicity testing. The cell suspension platforms used include petri dishes, 96 well plates, hanging drop plates, and 24 well plate PDMS molds. Each of these platforms was used to experiment with different combinations of spheroid characteristics, such as cell concentration and size, and data was collected concerning the compactness of the spheroid formed, measured by the sphericity. We found that PDMS-coated 96 well plates plated with a cell concentration of 5,000 cells resulted in spheroids after four days with the highest degree of compactness as calculated by an average sphericity of .958 ± .030.

1.0 Introduction

Parkinson's disease (PD) is the second most common neurodegenerative disorder in the United States, affecting between 750,000 and 1 million people annually. It is characterized by the loss of motor control attributed to the selective loss of dopaminergic neurons in the substantia nigra pars compacta. This neuronal loss causes resting tremors, bradykinesia, rigidity, and loss of postural reflexes. Genetic inheritance was commonly understood as the main link to Parkinson's disease, but recent studies uncover that only 15 to 20% of patients have a family history of Parkinson's. Therefore, it is likely that a majority of Parkinson's diagnoses are not genetically inherited but related to other factors, such as environmental stressors (Fernandez and Okun, 2009).

Most recently, Parkinson's disease has been linked to pesticide exposure without a clear mechanism for causation. Pesticides include various classes and subclasses of insecticides, herbicides, rodenticides, and fungicides that are released into the environment to kill or deter a target group of intruders. In 2001, approximately five billion pounds of pesticides were used worldwide, leading this deterrence to pose as a threat to many forms of life, including humans (Hatcher et al., 2008). Based on epidemiological studies, a pesticide at a certain exposure can accelerate underlying neurodegeneration without necessarily initiating the disease process. Bioaccumulation of these compounds could produce subtle toxic effects over extended periods of time and progress diseases like PD by increasing dopaminergic cell death making clinical symptoms visible (Hatcher et al., 2008).

Measuring toxicity levels of pesticides using *in vivo* and *in vitro* methods poses a challenge for researchers across the world. Establishing threshold values using rodent populations and engineered cells lines to compare induced exposure times to real life exposure

with pesticides is a correlation that is still in development. Currently, methods for measuring cytotoxicity include exposing populations of rodents to specific pesticides, observing the population for several weeks, euthanizing the population, and using brain sections to analyze toxicity levels (Thiffault et al., 2000; Manning-Bog et al., 2001). *In vitro,* cell lines can be exposed to a specific pesticide at different dosages, times, and combinations without harming living populations of test subjects.

Both *in vivo* and *in vitro* studies aim to analyze increased pesticide effects on neuronal cell viability, metabolic stress and oxidative stress. However, *in vivo* systems use large animal populations as test subjects, leading to ethical concerns, while standard *in vitro* systems only give a 2D perspective with a less physiologically relevant environment. Several studies have found morphological and molecular differences between 2D cultures and *in vivo* environments, leading to a necessary movement towards 3D cell culture. In 3D cell culture cells are encouraged to aggregate and form 3D microstructures known as spheroids, which enable greater cell to cell contact, imitating an *in vivo* system without an animal model.

Mn9D cells, a cell line created by the fusion of embryonic ventral mesencephalic and neuroblastoma cells, are widely used as a 2D *in vitro* model to study neurodegeneration mechanisms 2D (Fraley et al., 2010; Ghosh et al., 2005; Pampaloni et al., 2013). However, there are currently no methodologies for studying neurodegeneration in dopaminergic cells in 3D cell culture. In particular, no research has been done on Mn9D spheroid formation. Therefore, the goal of this project is to design a high throughput, 3D *in vitro* Parkinson's disease model as a standard system to measure neurodegeneration in dopaminergic cells after chronic exposure (hours) to an environmental stressor, such as a pesticide. An efficient system for studying the characteristics of neurodegeneration, using Mn9D spheroids, will allow scientists to more

effectively and specifically research the mechanisms involved in neurodegeneration in a physiological relevant environment, while diverging from animal testing.

2.0 Literature Review

2.1 Parkinson's Disease

Parkinson's disease is a common neurodegenerative disorder with no cure or proven strategy for slowing disease progression. PD is strongly associated with ageing characterized by motor dysfunctions such as bradykinesia, rigidity and tremor (Surmeier, 2007). Non-motor symptoms that occur in the disease include cognitive dysfunction, sleep disorders, psychiatric symptoms, and gastrointestinal dysfunction (Drolet et al., 2009). A small percentage (5%-10%) of PD cases are caused by monogenetic mutations, with the rest having no known etiology (Hatcher et al., 2008).

Although the pathology for these symptoms is unclear, PD has been connected to the selective degeneration of the dopaminergic neurons in the substantia nigra pars compacta (SNc), loss of dopamine input to the striatum, and formation of Lewy bodies (Chan, Gertler, and Surmeier, 2009; Hatcher et al., 2008, Betarbetet al., 2000). Dopamine is a neurotransmitter that plays a significant role in motor, cognitive, motivational, and neuroendocrine functions by inhibiting the transmission of nerve impulses in the substantia nigra, basal ganglia, and corpus striatum (Hisahara and Shimohamma, 2010). The loss of dopamine is responsible for motor symptoms exhibited by PD patients (Hatcher et al., 2008). Lewy bodies are abnormal inclusions in the cell soma and neurites of nerve cells comprised of the proteins ubiquitin- and alpha-synuclein, which is responsible for the progression of PD due to mutations of the PARK1 and SNCA genes (contains instructions for α-synuclein production), leading to deregulation of neurotransmitter release (Lotharius and Brundin, 2002; Hisahara and Shimohamma, 2010).

Motor symptoms are primarily connected to the loss of dopaminergic neurons in the SNc. Organelles responsible for the cellular regulation of calcium (Ca^{2+}) channels, like the mitochondria and the endoplasmic reticulum, have been linked to a compromised functioning of dopaminergic neurons. Metabolic and oxidative stresses on the cells lead to accelerated aging of neurons in the SNc, progressing PD in individuals (Chan, Gertler; Surmeier, 2009).

PD at a cellular level of a dopaminergic neuron disrupts SNc homeostasis, making neurons vulnerable to different genetic, cellular, and environmental factors that contribute to cell death over time (Figure 1). Mitochondria, ER, and α-synuclien are sensitive to homeostasis imbalance leading to a progression of PD. Lewy bodies can cause cell death by the aggregation of α-synuclein or misfolded proteins and reduced mitochondrial activity. Mitochondria can dysfunction causing oxidative stresses on the neuron leading to toxicity and neuronal death. Gene mutations impair functioning of specific proteins, calcium regulation, and endoplasmic reticulum function (Obeso et al., 2010).

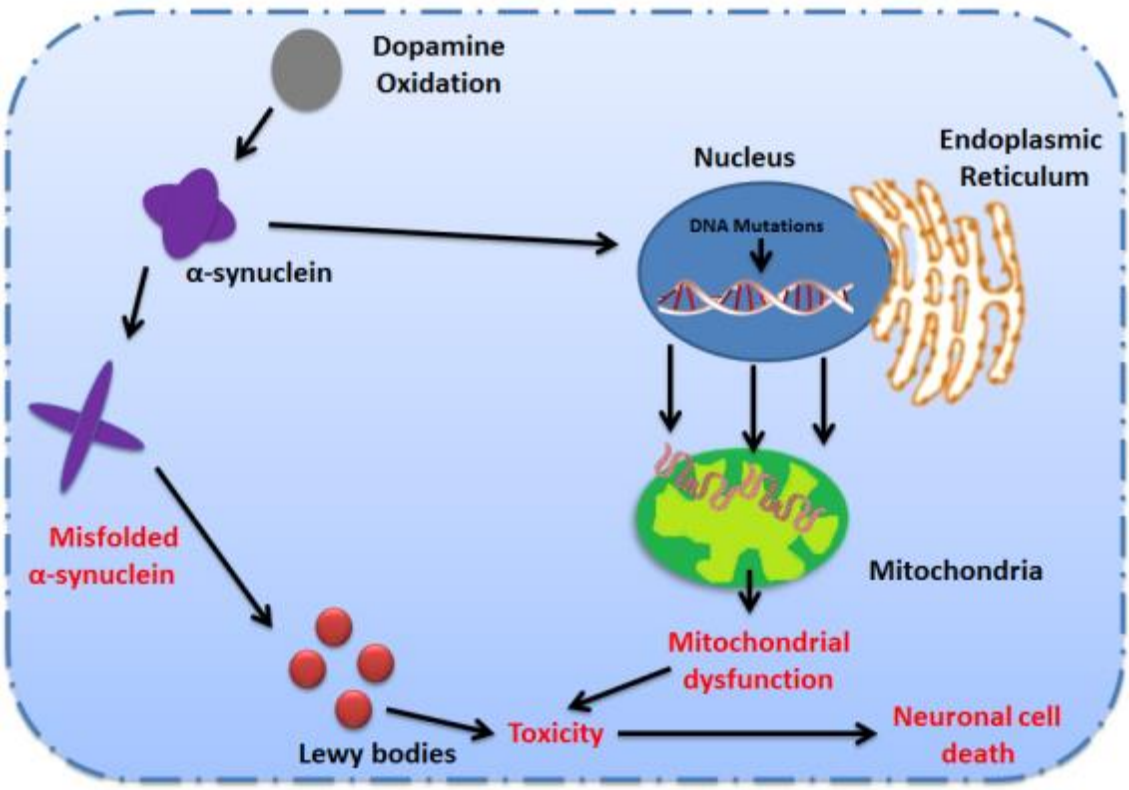

Figure 1. Schematic of mechanisms in dopaminergic neurons of the substantia nigra pars compacta in Parkinson's disease adapted from Obeso et al., 2010.

2.1.1 Calcium Dynamics of Parkinson's Disease

SNc dopaminergic neurons possess unique Ca^{2+} dynamics compared to most neurons in the body. While most neurons are voltage gated, opening only during periods of action potentials allowing small Ca^{2+} influxes, dopaminergic neurons in the SNc remain open nearly all the time to maintain autonomous activity creating large Ca^{2+} influxes, flowing through a concentration gradient. Ca^{2+} channels assist many cellular processes in enzyme regulation, gene expression, and programmed cell death. SNc neurons rely on Ca^{2+} channels to monitor activity and interaction with other neurons (Chan, Gertler, and Surmeier, 2009; Surmeier, 2007).

All the Ca^{2+} imported into the neurons must be rapidly sequestered to maintain functioning before being recycled out of the cell by the mitochondria and the endoplasmic reticulum (ER). Figure 2 shows the effect of external stressors increasing neuronal stresses. Neurons begin to have an up-regulation of Ca^{2+}, causing a 'Ca^{2+} overload.' The excess calcium begins to push its way into the mitochondria and endoplasmic reticulum, leading to the failure of these organelles, alterations of calcium buffering capacities, and exocitotoxicity (Marambaud et al., 2009; Surmeier, 2007).

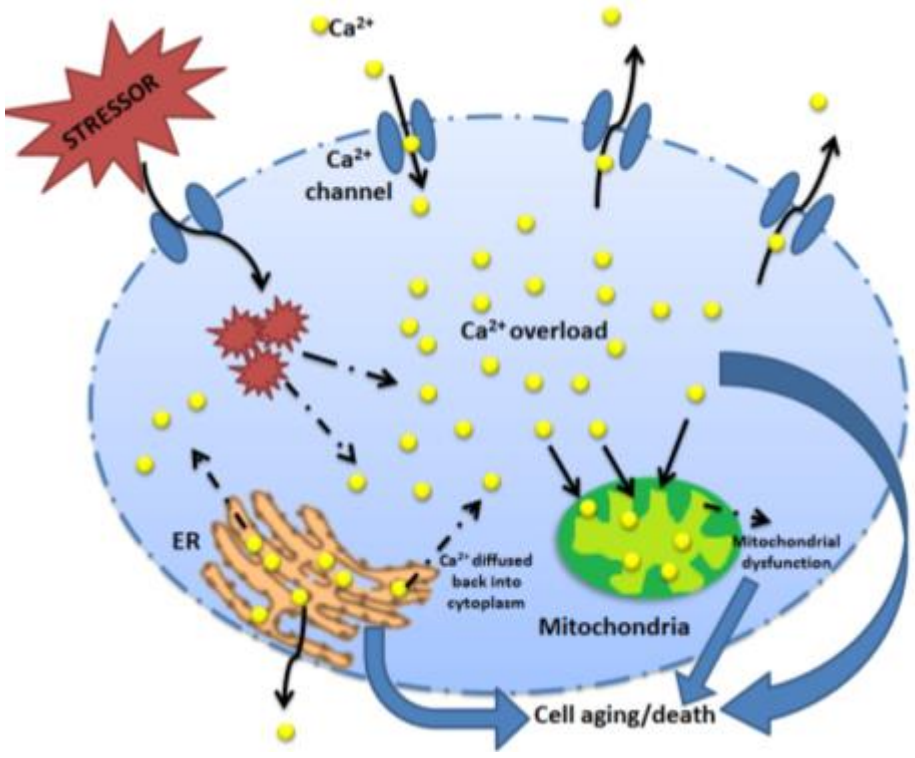

Figure 2. Calcium signaling in a PD brain adapted from Marambaud et al., 2009..

Maintaining calcium dynamics in dopaminergic neurons of the SNs creates metabolic stress on the cells, causing them to age faster and deplete at a higher rate (5-10% more per decade) than other neurons (Surmeier, 2007). The endoplasmic reticulum beings to lose its ability to properly fold and process important metabolic proteins, passing on through the

mitochondria, inhibiting its ability to generate ATP needed to maintain neuronal activity (Chan, Gertler, and Surmeier, 2009). Measuring internal calcium levels and observing morphology of organelles like the mitochondria and ER, can create a link between cytotoxicity levels and cellular failure to create threshold values of chemical compound safety levels. In the future these calcium pathways can be targeted to create therapeutic agents to offset neurodegenerative disorders (Marambaud et al., 2009).

2.1.2 Oxidative Stress in Parkinson's Disease

Oxidative stress in PD interferes with cellular functioning, leading to dopaminergic cell degeneration. The pathogenesis of PD can be characterized by the oxidative stress caused by mitochondrial dysfunctioning. Reactive oxygen species (ROS) lead to mitochondrial swelling and respiratory impairment. A dramatic increase in ROS as a result of mitochondrial dysfunction overwhelms cellular antioxidant mechanisms, and releases byproducts in the cytosol that create protein aggregates (α-synuclei Lewy bodies), leading to a higher rate of neuron depletion (Janda et al., 2012; Hwang, 2013).

Damaged mitochondria are accumulated, contributing to inefficient oxygen reduction causing increased ROS and reactive nitrogen species (RNS) formation. The oxygen imbalance inhibits the cell from detoxifying ROS and RNS and reactive species begin to target healthy mitochondria, preventing the cell's ability to clear our damaged mitochondria (Figure 3) (Sanchez-Perez, 2012).

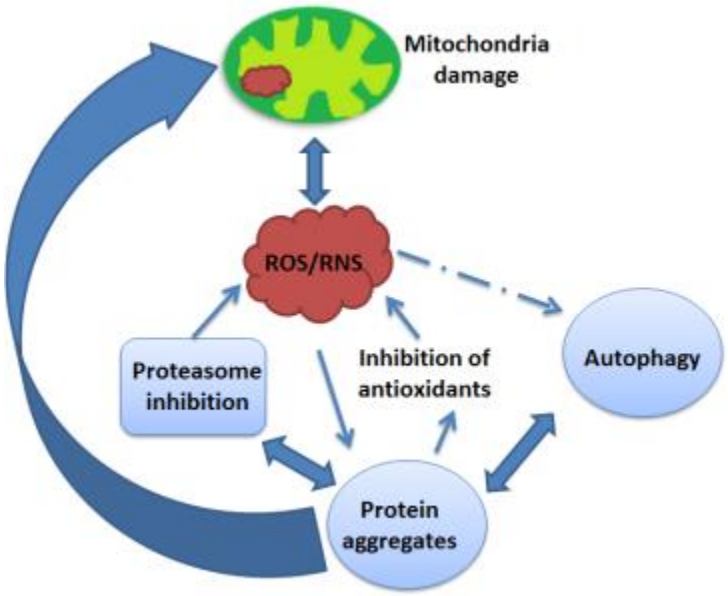

Figure 3. Mitochondria and ROS/RNS production adapted from Sanchez-Perez, 2012.

Increased ROS production and oxidative stress provides a link to environmental factors and PD. Recently certain toxins such as 1-methyl-4-phenylpyridiumrotenone, paraquate, and metamphetmaine have been linked to autophagy dysregulation (mutations of α-synuclein and disruption of electron transport chain) in dopaminergic neurons of the SNc. Oxidative stress is proven to induce excessive autophagy levels that lead to apoptotic or nanoapoptotic cell death (Janda, et al., 2012). Understanding how specific toxins interact with dopaminergic neurons though observations of ROS production, oxidative stress levels, protein concentrations, and cell viability can assist in monitoring and screening of cytotoxic compounds to prevent future neurodegeneration.

2.2 Pesticides

The Food and Agriculture Organization (FAO) of the United Nations define pesticides as "any substance or mixture of substances intended for preventing, destroying or controlling any pest, including vectors of human or animal disease, unwanted species of plants or animals

causing harm during or otherwise interfering with the production, processing, storage, transport or marketing of food, agricultural commodities, wood and wood products or animal feedstuffs, or substances which may be administered to animals for the control of insects, arachnids or other pests in or on their bodies" (FAO Corporate Document Repository, 2003). Consisting of over 1000 active ingredients marketed as insecticides, herbicides, and fungicides, pesticides are considered to be one of the main contributors to environmental contamination. Long-term contact with pesticides have also been linked to human health disorders including cancer, multiple sclerosis, diabetes, aging, cardiovascular disease, Alzheimer's disease and of specific interest for this project - Parkinson disease (Mostafalou, 2013).

2.2.1 Pesticides and Neurological Disorders

Several studies examine the relationship between pesticide exposure and elevated risk of chronic neurological disorders such as Alzheimer's and Parkinson's disease (Mostafalou, 2013). A systemic review and meta-analysis of 39 case studies, four cohort studies and three cross-sectional studies calculated summary risk ratios (sRRs) – the risk of an event in an experimental group compared to the risk of an event in a control group - for pesticide exposure and the late-on-set of Parkinson's disease. The four cohort studies analyzed pesticides as a risk factor for Parkinson's disease by focusing on incidence, cause and prognosis of the disease. Correlations were used to determine the absolute risk of a group of people developing Parkinson's disease. This was compared with the three-cross sectional studies that were used to determine prevalence of the disease by looking at the number of cases of PD in a population at a given point in time (Mann, 2003). A positive association between exposure to insecticides and Parkinson's disease resulted in a sRR of 1.5 (Van, Der Mark et. al, 2011). Elevated levels of pesticides have also been reported in serum of patients with Parkinson disease (Mostafalou, 2013).

Limited knowledge exists regarding the exact mechanisms that lead to degeneration in dopaminergic neurons as a result of pesticide exposure; however studies indicate oxidative stress and mitochondrial dysfunction in response to exposure play the biggest role (Mostafalou, 2013). For example, studies have been done exposing the pesticide rotenone, a natural insecticide, to rat. Rotenone inhibits complex I in the electron transport chain which induces oxidative stress in the rat's brains, leading to mitochondrial dysfunction and an increased level of ROS in the rat's dopaminergic neurons, similar to what occurs in PD patient's brain cells (Sherer, 2003; Panov, 2005; Betarbet, 2000). Paraquat, a world-wide used herbicide, has also been shown to interfere with the electron transport chain in dopaminergic neurons leading to increased ROS production, ATP depletion and cell stress (Janda, 2012).

Scientists are still in the early phases of piecing together the relationship between pesticide exposure and PD and until then the connection between the two will remain unclear. It is a relationship that is likely shaped by both genetic and environmental factors. In particular, researchers are interested in how chronic, low dose exposure to pesticides over extended periods of time (months or many years) can lead to PD (Kamel, 2013).

2.2.2 Confidor

In the 1990's there was a drive to produce highly selective pesticides that directly attack target pests. In response, a class of insecticides referred to as neonicotinoids (neonics) were developed (Malev, 2012). Neonics are synthetic derivatives of nicotine that bind to the nicotinic acetylcholine receptor, a nerve receptor in the insect brain. After binding, neonics causes nerve impulses to spontaneously discharge leading to neuronal failure and eventually insect paralysis and death (Imidacloprid Technical Fact Sheet, 2013). They are advantageous over other

insecticides because they can be readily absorbed by plants and then transported throughout their tissues, therefore targeting pest herbivores that consume the plant tissue (Goulson, 2013).

Scientists have recently become interested in imidacloprid (IMI), a neonictinoid and the second most widely used agrochemical in the world (Goulson, 2013). Known better by its commercial name, Confidor, evidence suggest IMI is killing bees, economically the most important group of pollinators worldwide using a similar mode of action (Malev, 2012; Oregon State University, 2013). As non-target organisms, bees ingest residues of IMI in pollen and nectar in treated plants (Laycock, 2012). When exposed to sub-lethal doses of IMI, they have been shown to experience reduced foraging, homing, and learning ability (Goulson, 2013).

There is fear that these insecticides could be causing harm to other non-target organisms such as humans. A limited number of studies have been done concerning IMI and neonictinoids in general and their effect on mammalian nicotinic acetylcholine receptors (nAChRs). nAChRs are important in the development and function of the human brain, therefore there is a need to understand IMI and its effects on neurons (Kimura-Kuroda, 2012). These effects could be better understood if experiments could be designed to compare the effects of IMI on dopaminergic neurons vs. well established pesticide models such as rotenone.

2.3 Current Methods

Methods used by researchers studying the neurodegeneration caused by pesticide exposure vary considerably in the neuronal models used, pesticide dosages and exposure times, and data collection techniques. These differences make it difficult to compare results due to the various methods used to cause and characterize the neurodegeneration in both *in vivo* and *in vitro* models.

2.3.1 *In Vivo*

Many *in vivo* studies are done on rats and mice to study how neurodegeneration affects an entire organism. Studying live animals allows researchers to better understand the mechanisms of neurodegeneration and how the body responds to pesticide exposure, such as behavioral changes and potential protective responses (Mangano et al., 2012; Marella et al., 2008; Tapias et al., 2010). A benefit to using animal models is the application of data about protective responses to potentially develop therapeutics to treat neurodegeneration (Tapias et al., 2010).

While using live animals to gain knowledge about neurodegeneration mechanisms has benefits, such as studying how other organs are affected by pesticides, psychological changes, and developing specific drugs based on protective reactions in the body, there are limitations to these animal models. For example, rats and mice can be exposed to a pesticide by intraperitoneal injections at varying dosages and injection frequencies. One study injected 1 mg/kg of the pesticide rotenone, while another study injected 10 mg/kg of paraquat 3 times a week for 3 weeks (Mangano et al., 2012; Tapias et al., 2010). Discrepancies in dosages and frequency of exposure make it difficult to compare results, even if using the same live animal model. Furthermore, recent studies suggest that rats may better represent the pathophysiological conditions of Parkinson's disease (i.e. neuronal cell death in the substantia nigra, Lewy body-like cytosolic aggregations, etc.) than mice (Marella et al., 2008). If rat models better represent neurodegeneration, then data from rats cannot be directly compared to data collected from mice. Additionally, some people believe there is an ethical need to transition away from the use of laboratory animals to study neurodegeneration (EPA, 2012; Garbarini N., 2010).

There are several reasons to transition away from animal models, particularly for pesticide testing. First, maintaining laboratory animals is very expensive and requires a lot of man power (Gabarini N., 2010). Some tasks involved with caring for laboratory animals include food, cleaning cages, transportation, and proper disposal to name a few. Second, there are considerable ethical dilemmas involved in lethal dosage (LD50) testing. LD50 testing is a standard procedure to assess the degree of toxicity of a pesticide (EPA, 2012). This procedure determines the dosage that kills 50% of the rat population that has been exposed to the pesticide. The animals (typically rats and mice) can be exposed to the pesticide through a number of methods including oral, dermal, and inhalation (EPA, 2012). There is a need to develop better tests that are more predictive of human health effects and less expensive than the current *in vivo* methods.

2.3.2 *In Vitro*

In vitro models, such as harvested cells, embryonic stem cells and genetically engineered stem cells, offer an alternative to expensive *in vivo* models. Harvested cells include neonatal rat cerebellar cultures, rat midbrain slices, etc., which allow researchers to study various aspects of isolated neuronal networks, particularly through measuring neurodegeneration by the extent of Ca^{2+} influx (Freestone et al., 2009; Kimura-Kuroda et al., 2012; Legradi, et al., 2011). Similarly, mouse embryonic stem cells (mESCs) can be used to study how neurodegeneration occurs in a complicated neuronal network. These cells can differentiate into various neuronal cells including neurons, astrocytes, oligodendrocytes, and radial glial cells (Visan et al., 2012). These cells are advantageous because the extent of differentiation can be easily analyzed using flow cytometry and they represent a complex neuronal network (Visan et al., 2012).

Instead of using a model for an entire, complex neuronal network, genetically engineered stem cells can be used to study a specific pathway. Examples of genetically engineered cells include Mn9D cells and F11 cells. Mn9D cells are a fusion of embryonic ventral mesencephalic and neuroblastoma cells, which are well-established as a model of dopaminergic neurons due to their large amounts of dopamine and tyrosine hydroxylase (Kim et al., 2007; Kang et al., 2012). Mn9D cells are widely used as an *in vitro* model to measure changes in Ca^{2+} dynamics in neurodegeneration mechanisms (Kim et al., 2007; Kang et al., 2012). Another in vitro model of neurodegeneration is the F11 cell line. F11 cells are a fusion of mouse neuroblastoma cell line N18TG-2 and embryonic rat dorsal-root ganglion (DRG) neurons (Fan et al., 1992). F11 cells have been used to obtain data concerning the specific toxic pathway of environmental stressors (Malev et al., 2012). Not only do these various *in vitro* models vary in their degree of complexity, but they also vary in the experimental setup used.

Recent studies report exposing cells to concentrations of pesticides that vary greatly. These concentration ranges included: 100μM, 10μM and 1μM of imidacloprid (Kimura-Kuroda et al., 2012); 5nM, 50nM, 200nM, and 1μM of rotenone (Freestone et al., 2009); 1nM, 3nM, 5nM, 10nM, and 20nM rotentone (Radad et at., 2008); and 10nM rotenone (Kang et al., 2012). Furthermore, these studies report exposure times that vary from 24-144 hours (Malev et al., 2012; Radad et at., 2008). The differences in how researchers cause neurodegeneration, and the differences in the concentration and duration of pesticide exposure complicate the analysis of the degree and mechanism of neurodegeneration.

Unfortunately, even the data analysis techniques used are very different too, which further clouds the pool of neurodegenerative knowledge collected by these studies. Analytical tools have multiple variables including fluorescent dyes and imaging techniques. Many studies

use immunohistochemistry to gather qualitative and quantitative data. Common immunohistochemistry reagents used in these analyses include tyrosine hydroxylase (Kim et al., 2007), Oregon Green BAPTA-1 (Talbot et al., 2012; Kang et al., 2012), Fluo-4-AM (Visan et al., 2012; Kimura-Kuroda et al., 2012), and Fura-2 (Freestone et al., 2009) in addition to many antibodies. These reagents are typically used to measure the change in Ca^{2+} dynamics after exposure to a pesticide. The fluorescent dyes bind to Ca^{2+} and then change color when excited by a xenon or argon laser at a specific wavelength (Freestone et al., 2009; Kimura-Kuroda et al., 2012). A high speed camera collects the changes in fluorescence and the images can be quantified using a Matlab or similar program to measure the behavior of the Ca^{2+}. Another data collection technique is patch clamping to measure the voltages of Ca^{2+} channels (Freestone et al., 2009; Kim et al., 2007). While this provides quantitative data, it is hard to compare to data collected using fluorescent dyes because the data can be quantified in different ways. The inability to compare the fluorescence data limits of knowledge available as a basis for future studies.

2.4 Improvements

Current studies have significantly contributed to the knowledge of neurodegeneration and its mechanisms, however there are several improvements that could be made to accelerate data collection. First, a standard cell line that closely represents the neuronal network in humans would ensure that the data collected is applicable to finding solutions to neurodegenerative disorders. Second, an established combination of pesticide dosage and exposure time that mimics the neurodegeneration that occurs in humans would reduce the time needed to prepare the study, leaving more time and requiring fewer resources to understand the mechanisms involved in neurodegeneration. Third, an established data collection and analysis process would reduce the

number of variables that may cause differences in data. Fourth, a standard output would allow for easy comparison between studies. For example, Ca^{2+} voltages from patch clamping are difficult to compare to Ca^{2+} influxes from fluorescent dyes, but if a conversion could be made that allowed for all studies to report the same output the comparison would be much more meaningful. Fifth, an overall reduction in amount of cells or animals, pesticides, fluorescent dyes, etc. used would decrease the cost of studying neurodegeneration.

In addition to these limitations, there is evidence that 2D cell culture systems are not representative of real tissue. Several studies have found significant morphological and molecular differences between 2D cultures and *in vivo* studies, and as a result, support the transition to cultivate cells in 3D rather than 2D (Fraley et al., 2010; Ghosh et al., 2005; Pampaloni et al., 2013). The benefit of using a 3D cell culture system is increased cellular interaction due to the formation of cellular spheroids, which are round clusters of cells that are formed spontaneously by the clumping of isolated cells (Figure 4) (Pampaloni et al., 2013).

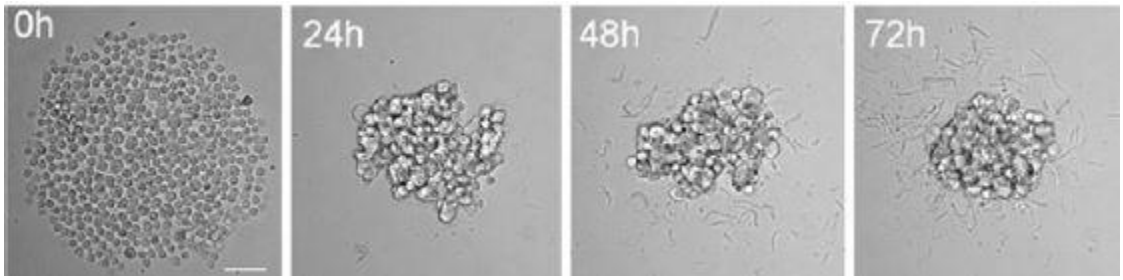

Figure 4. Formation of a spheroid

Traditional 2D systems contain cells on flat Petri dishes that only allow moderate cell-to-cell contact, whereas 3D systems enable greater contact between cells by utilizing a matrix scaffold, hanging drop plates, or other mechanisms to form spheroids (Table 1).

Table 1. Comparison of 2D and 3D Cell Culture Techniques

Cell Culture System	Platform Used	Cell Structure
2D Petri dish	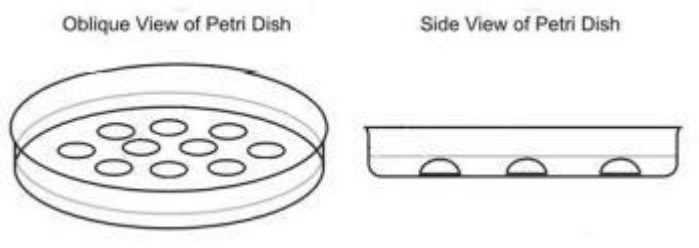	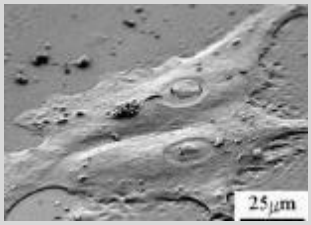
3D Matrix scaffold	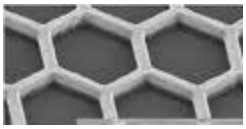  	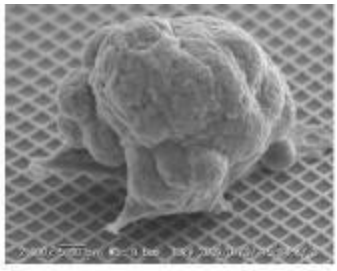
3D Hanging Droplet Plates		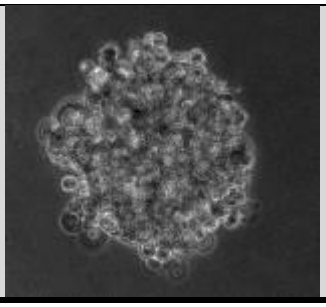

Due to the decreased cellular contact, 2D systems are inferior to 3D systems in mimicking the microstructure, dynamic mechanical properties, and biochemical functionalities of living organs (Astashkina et al., 2012; Huh et al., 2011; Pampaloni et al., 2013; Rimann & Graf-Hausner, 2012). Thus, data collected via 2D systems may not accurately represent the cellular and tissue interactions that occur in the human body (Astashkina et al., 2012; Huh et al., 2011; Pampaloni et al., 2013; Rimann & Graf-Hausner, 2012). By increasing cellular contact, the

formation of spheroids in 3D cell culture systems provide data that is more physiologically relevant than traditional 2D cell culture systems.

3.0 Project Strategy

The goal of this project is to develop and design an optimal 3D system with the ability to measure neurodegeneration by screening cytotoxicity in Mn9D spheroids after exposure to environmental stressors. This chapter defines the steps and methods used to relate the objectives and constraints of the project back to the client statement. It helps to organize the project goals and sets up a strategy for their timely completion.

3.1 Initial Client Statement

The clients at the University of Nova Gorica provided the project team with a brief project description as stated below:

> *Develop a high throughput in vitro process to screen cytotoxicity after exposure to varying doses and exposure times of pesticides in dopaminergic neurons as a model for Parkinson's disease.*

3.2 Design Parameters

Gaining an understanding of the initial client statement allowed the team to define objectives, constraints, and functions pertaining to the final design. Objectives were defined as the desired performance characteristic to be met by the final design. Design constraints were identified as limitations on the development of the design, and functions defined as what the design was to perform.

3.2.1 Objectives

After discussing the initial client statement and understanding the needs of the project the team developed the following objectives and ranked them using a pairwise comparison chart (Appendices A and B):

1. **Reproducible:** The design consistently produces a spheroid in each well/drop with an average diameter of 250 – 500 µm.
2. **User Friendly:** The designed process can be implemented into various labs interested in the mechanisms of measuring toxicity of neurodegeneration. The process is user friendly in the sense that the materials used are easily obtained, the methods can be performed in most labs, and the results can be analyzed by any user.
3. **Scalable:** To create a scalable *in vitro* process, the team looked into designing a high throughput and efficient system. The process should enable the analysis of a large quantity of data and identify multiple results in minimal time. This scalable design can also test varying dosages, concentrations, and exposure times of specific pesticides.

After defining primary objectives, secondary objectives were identified to gain a more in-depth understanding of the design. For reproducible the secondary objective – optimal spheroid geometry – was defined. To run consistent experiments with the spheroids, each spheroid should be similar in size and shape. As a result it is important that the design continuously reproduces spheroids as similar to each other as possible. In particular, it is important that the spheroid diameter falls into a range between 250 and 500 µm. If any larger, there is a high probability the spheroid will develop a necrotic core – cell death at the inner core- due to the inability of nutrients to diffuse to the center of the spheroid (Vinci, 2012).

The objective ranked second was user friendly. The sub-objectives chosen were: easily analyzed and easy attainability of materials. For the process to be user friendly so others can practice it, the design should be built so that anyone using this process can set it up and obtain results that can be understood and analyzed. It is also important that low cost and readily available materials are used so any lab in the future would be able to successfully perform this

process.

The objective ranked third was scalable. The sub-objectives are: high-throughput and efficient. A high throughput process will create many spheroids for toxicity testing in minimal time. This way various pesticides screenings can be run to output toxicity results. The design should also be as efficient as possible with a small number of components involved. A procedure with a small number of components will in turn save time and money.

3.2.2 Constraints

Design constraints were identified to set limitations on the development of the design. The first constraint is that the design must be *in vitro.* The client is looking to move away from *in vivo* testing which is surrounded by ethical concerns. It is also believed that using human engineered cell lines is a better representation of the mechanisms taking place in the body.

The design process was under strict time constraints and limited in readily available materials. With seven weeks to complete the project, time management and scheduling of each experiment is imperative to the progression of the teams design. Working in a new and developing lab, there is limited access to materials on hand. As a result it will be important to develop detailed plans in advanced so that materials can be ordered with their delivery time factored in.

Concerning the spheroids themselves, they must not exceed 500 μm in diameter. If the spheroid exceeds this size then the proper amount of oxygen and nutrients will be unable to diffuse throughout the entire spheroid and there is a potential of it forming a necrotic core. (Wallace & Guo, 2013).

3.3 Revised Client Statement

A final client statement was developed after finalizing the objectives and constraints of the project:

> *Develop a high throughput in vitro process to create 3D spheroids using Mn9D cells as a model for Parkinson's disease and can screen for cytotoxicity after exposure to varying doses of pesticides.*

3.4 Project Approach

To meet the needs of the client statement, there were a number of goals that the design team needs to accomplish. These goals are focused around the time and budget of the project. The project needs to be completed by mid-December 2013 and stay within a budget given to the team by the clients. A Gantt chart and Work Breakdown Structure were created to keep the team on task, as shown in Appendices C and D. Background research, brainstorming and client's recommendations will be used when developing design alternatives and running experiments.

4.0 Design Alternatives

The team considered several aspects when designing the approach to create novel Mn9D spheroids. The team conducted a needs analysis to ensure that the design alternatives would incorporate the most essential and necessary components of the design. Functions and specifications were considered to make sure designs completed all the necessary purposes to successfully and consistently form spheroids. The team valued spheroid formation as the most important design aspect and considered several design alternatives to form these spheroids based on different approaches, such as: conventional hanging drops, hanging drop plates (Perfecta3D hanging drop plate), Shrinky Dinks, 3D printed mold for PDMS plates, and hydrophobic coatings of well plates/tops of petri dishes.

4.1 Needs Analysis

To design an optimal process to create Mn9D spheroids as a model for cytotoxicity testing, the project team and client discussed which design ideas were crucial for the success of the design and which ideas were desirable, but not necessary. After discussing the goal of the project with the client, the project team categorized each idea as a need or want (Table 2).

Table 2. Needs vs.wants

Needs	Wants
Form spheroids	Minimal pipetting
User friendly (at client's lab in Slovenia)	As many drops as possible
Maintain cell viability	Conduct analysis assay on same plating device
If necessary, allow for transfer of spheroids with minimal damage to morphology	
Easy imaging	
Easily change media	

The most important need is the ability to form spheroids. If the process is unsuccessful in forming spheroids from Mn9D cells, then the rest of the process is irrelevant. Second, the process must be user friendly such that it can be performed with the equipment available in the client's lab in Slovenia. Third, the process must maintain cell viability because it can take up to seven days for the cells to aggregate into spheroids. The cells must stay alive throughout the process from spheroid formation to toxicity analysis. Fourth, if transfer is necessary, the spheroids must be easily transferred to a 96 well plate or similar device for the toxicity assays and analysis. Therefore, the spheroids must be easily accessible and transferred using a method that does not disrupt the spheroid. Fifth, the process must allow for easy imaging, so the spheroids grown in a device that allows imaging to be performed by a microscope. This step is important for observing the spheroids formation. Sixth, the process must allow for easy access to the cell media. The cells require the addition of new media to provide nutrients and the keep the cells from drying out.

In addition to the needs of the design, there were several ideas that would improve the functionality of the process, but would not lead to failure if omitted from the design. Minimizing the amount of pipetting would be ideal throughout the process. Limiting the amount of pipetting reduces the risk of contamination and disruption of the spheroids. The project group would like to design a process that outputs as many spheroids as possible, but decided that it was more important to develop a precise and reproducible system before attempting to make the process high throughput. The optimal process of spheroid formation would include the ability to conduct the analysis assays on the same device where the cells were plated to form spheroids. This would eliminate the need to transfer the spheroids, therefore reducing the risk of disrupting the spheroid

geometry. Also, this would save money by reducing the amount of materials necessary for analysis. These wants were kept in mind as the project team explored design alternatives.

4.2 Functions and Specifications

After defining the objectives and constraints, the project team moved forward to define the functions, means and specifications of the design. The morphological chart (Table 3) demonstrates and outlines the potential design alternatives based on the various functions and means that the project team brainstormed.

Table 3. Morphological Chart

Functions/Means	1	2	3	4	5
Form Spheroids					
- **Cell Concentration**	1,000	2,500	5,000	7,500	
- **Type of Plate**	96 well plate	Petri dish	Hanging drop plate	Shrinky dink	24 well PDMS mold
- **Matrigel concentration**	None	0.1%	1%	5%	
- **Surface modification**	HEMA	PDMS	Agarose		
Maintain cell viability	Media exchange via perfusion system	Manually remove media and add fresh media			
Minimize evaporation	PBS	Media	DI Water		
Allow for easy transfer of spheroids	Eliminate the need to transfer spheroids	Add media so drop falls	Pipette and resuspend		
Allow for easy transfer of plate	Automated system	By hand			

Table 3 illustrates the numerous combinations that can be used to create design alternatives. The process of forming the spheroids can be done by varying parameters: cell concentration, type of plate being used, surface modification, and addition of scaffold, extracellular matrixes or basement membranes to help cell binding and increase spheroid compactness.

Other critical functions for the success of the design are maintaining cell viability, minimizing evaporation, and allowing for the easy transfer of individual spheroids and plates of spheroids. Spheroids must remain hydrated to keep cells viable. They can be kept hydrated by using a perfusion system or manually removing the media and replacing it with new media. Spheroids must also be able to be transferred for exposure and analysis. The best way to approach this function would be eliminating the need all together so that the device itself allows for this; however another option would be developing careful pipetting techniques.

To further define the team's functions, the design team came up with specifications for each function (Table 4).

Table 4. Functions and Specifications

Functions	Specifications
Form	• Diameter between 250 – 500 µm • Drop of media < 50 uL
Maintain cell viability	• Cells must live for 3-5 days • 50% viability
Minimize evaporation	• Reservoir containing 1-2 mL liquid
Allow for easy transfer of spheroids	• Spheroid diameter should not spread after transfer
Allow for easy transfer of plate	• 50% of Spheroids remain undisturbed

Table 4 provides more specific qualities of the functions for the design to adequately meet the needs of the client. Through defining the functions, means and specifications, the project team developed feasible design alternatives to achieve the client's goal.

4.3 Design Alternatives

4.3.1 Forming Mn9D Spheroids

The formation of the Mn9D spheroids is the most important step in the process. Because there haven't been any published studies that formed spheroids from Mn9D cells, the project team had to determine the best conditions to create such a spheroid. The project team varied the concentration of cells and matrigel added to each spheroid to determine the most successful method of spheroid formation. The concentrations tested were 1,000, 2,500, and 5,000 cells per spheroid. The project team needed to test several concentrations because the ideal concentration varies depending on the cell type used, and Mn9D cells have not yet been experimented with for spheroid formation. The project team compared the results of the spheroid formation with a control of a standard 96 well plate coated with polylysine plated with Mn9D cells. The protocol for plating the 2D cells can be found in Appendix E.

4.3.2 Spheroid Formation with Petri Dish

Petri dishes are an inexpensive and straightforward method to create hanging drops and readily available in many labs, including the University of Nova Gorica. Therefore, we proposed to create spheroids by making hanging drops on small petri dishes with four drops per plate to ensure the drops would not interfere with each other and allow all drops to be clearly labeled and organized. Keeping smaller plates with four drops per plate allows for the team to keep better track of drops and spheroid formation during imaging, limiting the chance of mislabeling images

and inability to locate spheroid under the microscope. However, petri dishes come in a variety of sizes with potential to scale up to larger dishes and produce more hanging drops on a single plate at one time (Figure 5).

Figure 5. Variety of petri dish sizes that can be used for hanging drops.

A drop of approximately 40µL is pipetted carefully onto the top of a petri dish that is face up. A 40µL drop can control the cell concentration by counting cells and diluting the media to a certain concentration. The drops can hold 2,500-25,000 cells per drop enabling various spheroid masses to form to resemble different biological tissues and 3D structures. After pipetting drops, the lid is flipped over quickly to suspend the drops and allow gravity to aggregate the cells into a spheroid. A schematic of the droplets can be seen in Figure 6.

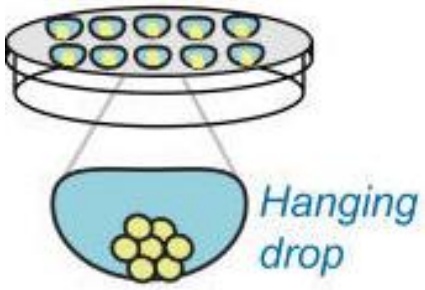

Figure 6. Schematic of hanging droplets on a petri dish to create spheroids.

Using a petri dish is simple, yet effective because they maintain cell viability and can be easily imaged. The bottom portion of the dish can be filled with water or PBS to keep cells from

drying out and evaporating. The lid can also be flipped back over without highly disturbing spheroids after 48 hours to replenish drops with fresh media. The protocol for plating drops on petri dishes can be found in Appendix F. After four to seven days, when spheroids are formed, more media can be added to each drop until the maximum weight for spheroid suspension is exceeded and it can fall into the dish to run cell viability and cytotoxicity assays.

4.3.3 Hanging Drop Plate

There are many devices on the market that have been designed in order to assist in optimal spheroid development. The University of Nova Gorica currently has access to a Perfecta3D® Hanging Drop Plate kit. The team decided to include the kit as part of our design alternative by testing how well the plate is able to form spheroids with Mn9D cells. The device consists of 3 major parts: the lid, the hanging drop plate itself, and a tray on the bottom (Figure 7).

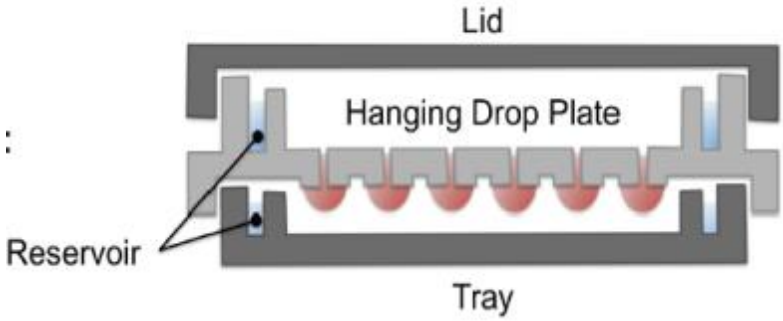

Figure 7. Layout of hanging drop plate consisting of lid, hanging drop plate, and tray with reservoir.

Cell suspensions of 30-50 μL with concentrations varying from 2,500 to 25,000 cells/mL can be separately pipetted into each well located as part of the hanging drop plate piece in the center (Figure 8) and PBS, water, or another buffer solution can be placed in the reservoir to

keep the cells hydrated once the plate is placed in the tissue culture incubator. The protocol for plating the hanging drop plate can be found in Appendix G.

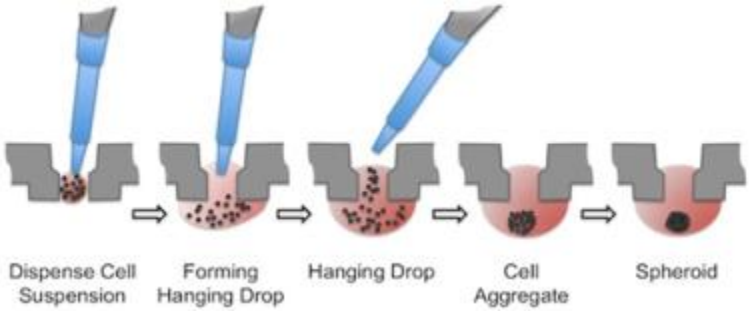

Figure 8. Method to manually pipette cell suspension into each well in the hanging drop plate.

Media can be added to and removed from each hanging drop daily using a pipette to aspirate the old media out and then replace it with fresh media. The amount of media to be added or removed varies with experimental conditions and cell type and the team will need to figure out which process works most efficiently and creates well packed and viable Mn9D spheroids.

The Perfecta3D® Hanging Drop Plate kit has successfully been used to culture 3D spheroids of over 30 different cell types and as a result appears to be a good option to test with Mn9D cells. When using the Perfecta3D® Hanging Drop Plate the team needed to experiment with the concentration and size of the cell suspension, as well as decide on whether it will be useful to use extra cellular matrix proteins in order to increase cell aggregation and spheroid formation, as described in the biological design section.

The Perfecta3D® Hanging Drop Plate kit is unique because it contains a receiving plate that can be used for direct analysis. The spheroids are collected by placing the receiving plate below the hanging drop plate. A small amount of fluid is dispensed into the hanging drop to push out the spheroid into the receiving plate as seen in Figure 9. Various assays can then be

performed and analyzed with the collected spheroids in the receiving plate. This eliminates the need to transfer spheroids to multiple other plates and risk harming or destroying the spheroid (3D Biomatrix, 2013.)

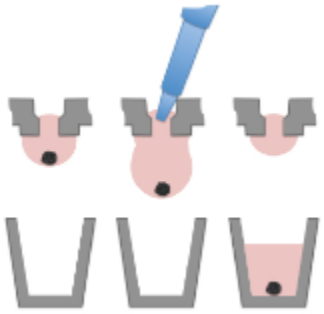

Figure 9. Method to transfer formed spheroids from hanging drop plate to receiving plate.

4.3.4 Shrinky Dink Plate

A children's toy called Shrinky Dinks has recently been used to create microfluidic devices, as well as hanging drop plates for 3D cell culture. Shrinky Dink paper is biaxially oriented polystyrene thermoplastic sheet with heat sensitive properties that cause it to shrink to about 63% of its original size with heights up to 80 µm (~500% increase), but still maintain shape during PDMS curing (Grimes et al., 2007). Shrinky dink paper is inexpensive and can be printed using a standard laserjet printer and shrunken down using a conventional oven or toaster over. The entire process eliminates the need for photolithographic techniques and clean room access, which some labs may not have access (Grimes et al., 2007; Chen et al., 2008).

Using Shrinky Dink paper micro-scale devices can be created on a much larger scale using a program as simple as Micrsoft PowerPoint or more complex like Solidworks to create a pattern. The pattern is then printed using a standard printer and the darkness of the ink determines the height of the Shrinky Dink extrusions. The paper, if aligned appropriately, can be

run through the printer several times to increase extrusion height, providing variability in well and channel depth for hanging drop plates and microfluidic devices (Grimes et al., 2007). The device can be sterilized using isopropanol, acetone, distilled water, and air (Chen et al. 2008). Schematics of these devices are displayed in Figure 10 (Grimes et al., 2007; Chen et al. 2008).

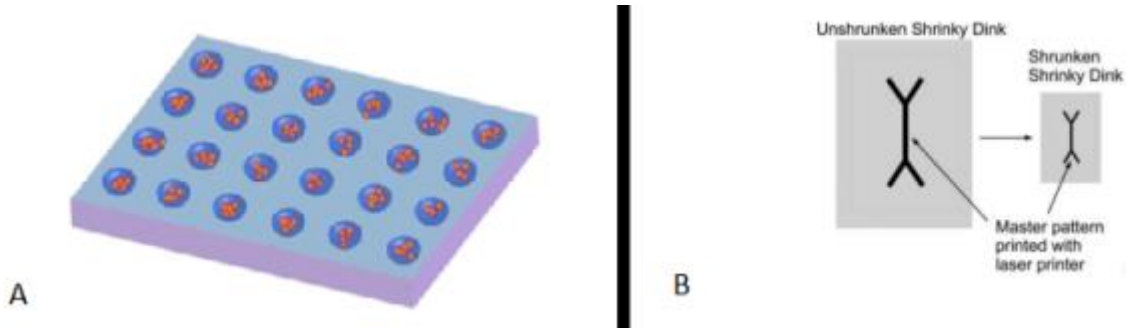

Figure 10. Schematicof (A) Micro-well plate and (B) Microfluidic device using Shrinky Dinks paper.

Once the Shrinky Dink mold is prepared and cleaned, PDMS is poured over the mold to form the micro-plate. The plate can be printed and designed with as many or as few wells as desired. A Shrinky Dink Plate create by Chen et al., was able to plate between 25 and 35 cells per well, and the PDMS micro-plate was made small enough to fit inside a 50 mL centrifuge tube. The Shrinky Dink plate is placed in a petri dish filled with media, allowing media to be extracted and replensihed with a single pipetting motion for each without disrupting spheroids (Chen et al., 2007). The protocol for plating the Shrinky Dink can be found in Appendix H. Figure 11 displays the process of designing a Shrinky Dink plate as developed by Chen et al.—(1) is the original printed paper, (2) shows the shrunken device mounted to a glass slide, (3) displays PDMS being poured onto the mold, (4) is the final PDMS mold made from the Shrinky Dinks, and (5) shows embryonic stem cell spheroids from a Shrinky Dinks drop plate (2007).

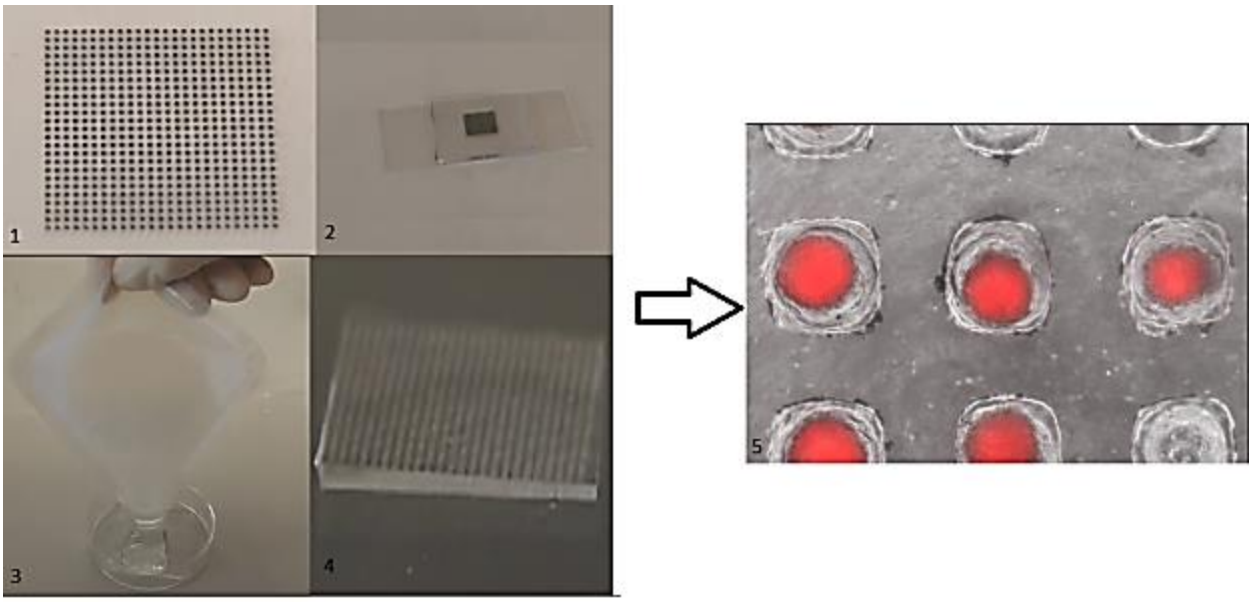

Figure 11. Fabrication of fabricating a micro-plate hanging spheroid device (1-4) and the resulting spheroids (5).

Printing a design with several wells makes the system more high throughput. One mold can be casted with PDMS several times to create a large amount of wells to run samples at a lower cost and use fewer cells. The micro-plate is placed in a centrifuge test tube and centrifuged to force all cells into wells. The centrifuge step eliminates the need for laborious pipetting of a standard 96-well plate for hanging drops. Utilizing the Shrinky Dink device would allow for consistent droplet size/shape, multiple spheroids at a time, a rapid way to manufacture well plates, and save the time of ordering new plates, pipetting, and complicated change of cell media.

4.3.5 Hydrophobic Coatings: PDMS

One of the major problems with hanging drops on petri tissue culture dishes is that the drops can be easily disturbed. This causes them to spread out and lose form or fall off the top of the dish. As a design alternative the team suggested coating the top of the petri dish with PDMS, a hydrophobic material, that would allow for the creation of firmer and more round drops. These

drops would hold their shape better and, as a result, the spheroid could easily sit in the center of the drop. The shape of the drop would encourage the spheroid to form a similar, compact shape.

Because cells have been shown to have low attachment rates to hydrophobic materials (Ratnayaka et al., 2013), the project team also looked into making a device out of PDMS and coating the bottom of petri dishes, 24 well plates, and 96 well plates with PDMS. Protocols for coating petri dishes, 24 well plates, and 96 well plates can be found in Appendices I-K.

4.3.6 Hydrophobic Coatings: Agarose

Agarose is another hydrophobic material that has been used to create spheroids due to its hydrophobic surface. Cells are unable to adhere to the agarose and, as a result, are encouraged to attach to each other (Friedrich, J et al, 2009). Similar to the PDMS coating, an agarose coating is placed on the bottom of a 96 or 24 well plate and the supernatant is pipetted on top. A 1% agarose coating is created mixing agarose powder with deionized water. The mixture is heated until boiling and coated onto a cell culture dish of choice. Once it has cooled down a layer will form on the bottom of the plate and the cells can be cultured. The protocol for coating 24 well plates and 96 well plates with agarose can be found in Appendices L and M.

4.3.7 3D Printed Molds

The University of Nova Gorica is limited in its resources as the lab is in its early stages. To eliminate the disposal of several petri dishes and well plates after each experiment or waiting to purchasing expensive commercial hanging drop plates, the design team proposes to cast custom made plastic molds with PDMS to create smaller multi-well plates for spheroid formation. The mold is reusable, designed once using CAD and then printed with a 3D printer. The PDMS can simply be mixed in the lab each time it needs to be used and disposed of afterward each experiment.

The team designed five variations of a similar mold using SolidWorks. Through a relationship established with the International Center for Theoretical Physics (ICTP), the molds were each 3D printed on either an Ultimaker or MakerBot 3D printer (Figure 12).

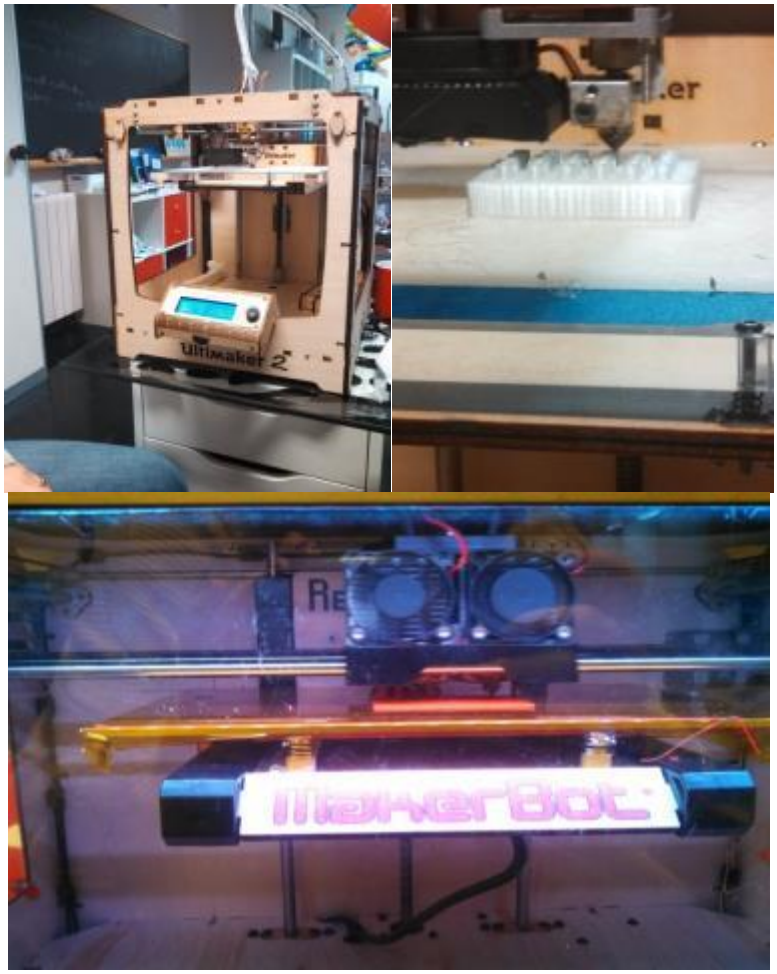

Figure 12. Set up and 3D printing of designed molds using the MakerBot at the ICTP in Trieste, Italy.

Each design was created from Acrylonitrile butadiene styrene (ABS), Polylactic acid or polylactide (PLA), and Polyethylene terephthalate (PET). The PDMS plate must fit in a standard sized petri dish so the molds were designed to be 40 mm x 60 mm. A sleeve is placed over the base to hold in the PDMS as it hardens. A spot is marked on the sleeve as to how high to fill the mold with PDMS so that it does not become too thick close the petri dish once the PDMS plate is

placed inside. Two variations of a rod-well plate were also designed to use less PDMS, fit over a 24-well plate, and allow for easy removal and cleaning of the mold. Table 5 allows for visualization and specifications of each design. (Note: CAD drawings can be found in Appendix M).

Table 5. 3D Printed PDMS molds designed by the team and printed at the ICTP.

Mold Type	3D Printed Mold	Description
Pyramid Well	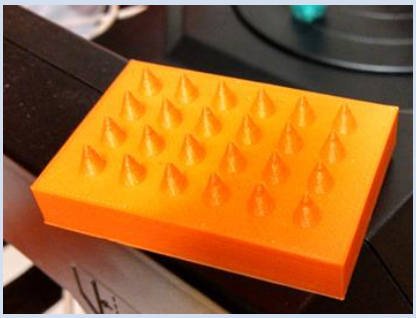	The first shape consists of 24 wells in the shape of a pyramid. This shape leaves the smallest (of the three) space in the bottom for cells to aggregate. The shape is modeled after Aggrewells 3D plate (STEMCELL Technologies, 2013).
Round Well	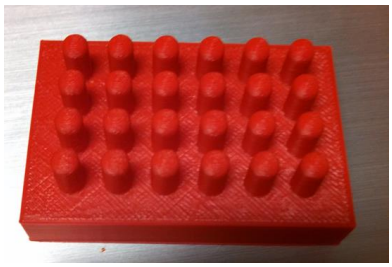	The second shape consists of 24 wells with bottoms in a shape similar to that of a 96 well plate. However, based upon data from an article written by Ratnayaka et al. each well is 5 mm in diameter (2013). The article used PDMS in a regular 96-well plate to create holes of similar size for 3D cell culture.

Truncated Cone Well	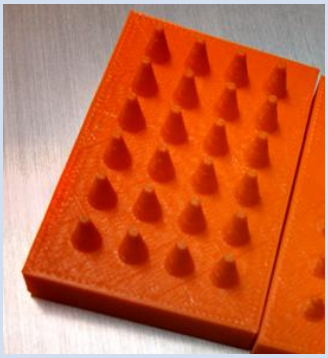	The final shape is a variation between the two. The well is in a shape similar to the pyramid bottom, however it has a flat bottom instead of a pointy one.
Sleeve Covering Base	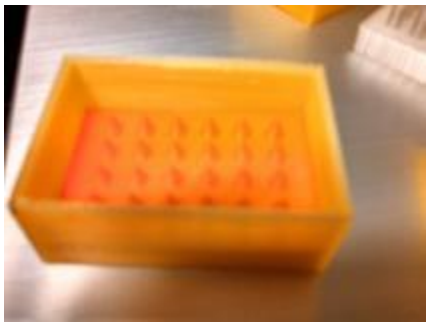	This picture allows the sleeve that covers the base of the mold to be visualized. The sleeve has no bottom allowing it to easily slide off the mold once the PDMS has hardened.
Rod-well Cone	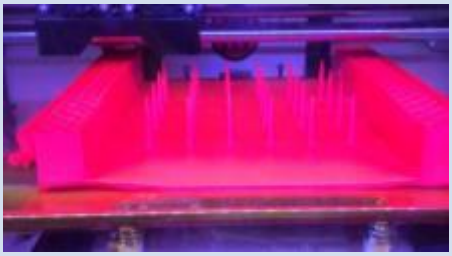	The rod-well cone plate fits over a 24-well plate filled with PDMS. The 5mm extrusions from the base create smaller wells within the 24-well plate. It allows for easy removal and a small, narrow area for spheroids to form.
Rod-well Round		The rod-well round plate fits over a 24-well plate filled with PDMS. The 5mm extrusions from the base create smaller wells within the 24-well plate. It allows for easy removal and a small, rounded area to encourage more rounded spheroid formation.

As mentioned above, the PDMS plates were designed to fit into a standard size petri-dish. This would allow it to be surrounded by media or PBS and then covered, to prevent contamination and drying out of wells. The PDMS plate could easily be centrifuged to better place the cells in the center of each divot and then placed in the incubator to allow time for cell growth and aggregation. The rod-wells could also have the well of the 24-well plate filled to capacity to easily change media and keep the cell hydrated.

The mold could continuously be reused to make PDMS dishes to plate the supernatants. PDMS has been used in many microfluidic and 3D drop hanging devices due to its transparent properties that allows its contents to be easily visualized under a microscope. PDMS is also easy to mold and inexpensive compared too many other lab materials (Guilhem, 2013). A protocol for making the PDMS molds can be found in Appendix N. Figure 13 shows a simple procedure of how a PDMS replica can be made from a mold and placed on a plate for cell loading and viewing. Examples of the team's PDMS molds can be seen in Table 6.

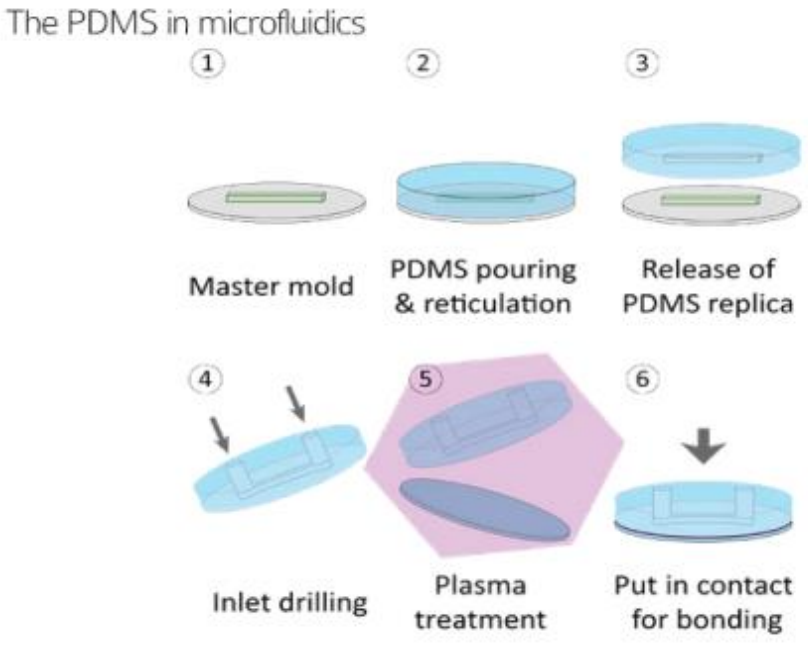

Figure 13. Simple outline of how a mold can be used to make a PDMS microfluidic device.

Table 6. Examples of finish PDMS molds created by the design team.

Mold Type	PDMS Mold
Truncated Cone Well	
Rod-well Round	

It is important to note that the current molds are on a millimeter scale. If given more time, the project team would have liked to scale down the mold to a nanometer scale such that it would be more efficient and high throughput. The project team would have ideally created smaller divots on a more compact device, similar to what is seen with Microtissues® device in Figure 14. The device can make hundreds of spheroids in a single pipetting step, and allows for the shape and size of each spheroid to be controlled. Furthermore, the project team would have

added a well that keeps the media from evaporating and an easier way to adjust the amount of or change the media in their design (Sigma-Aldrich, 2013).

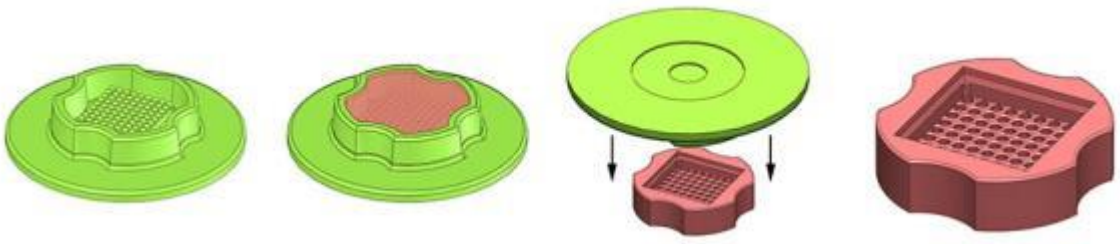

Figure 14. Example of Microtissues® high-throughput mold.

4.4 Experimental Methods

After the design alternatives were established, the design team began experimenting using numerous methods. The methods of cell culturing, cell counting, cell splitting and cell plating are all important processes needed to perform prior to testing the team's design alternatives. These processes are important for obtaining the cell concentrations and volumes used to create spheroids using the team's design alternatives.

4.4.1 Cell Culture and Spheroid Formation

Arriving at the lab in Slovenia, the design team was given a three plates of cells in which were used throughout the two months. To provide these cells with the correct nutrients to keep them alive and growing, cell culturing must be performed at least once every three days. Cell culturing is a process of numerous steps that involve collecting the current media, washing the cells, trypsinizing to detach cells from the plate/dish, incubating them and then centrifuging them to collect the healthy cells. Once that has been completed, new media is added to the cells and mixed together and they are then replated on a petri dish. Detailed protocols for preparing media and cell culturing are shown in Appendices O and P.

As shown in the design alternatives, cell concentration is very important, as the spheroids must remain in a certain microliter range for the entire spheroid to obtain the correct flow of nutrients. To determining the cell concentrations, it is necessary to count the cells. After culturing the cells, 10 μL of the cells are placed in a hemocytometer to count using a microscope. The process of counting cells using a hemocytometer is described in Table 7.

Table 7. Calculations for Cell Counting

Calculation	Description
132 + 169 + 210 + 126 = 637	Added the number of cells counted in each of the four squares of the hemocytometer.
637 / 4 = 159 average	Divided the total number of cells by the total number of squares to calculate the average number of cells per square.
159 / 0.1 = 1,592	Divided the average number of cells by the 0.1 dilution.
1,592 (10000) = 15,925,000 cells per mL	Multiplied by the volume of the hemocytometer to calculate the total cells per mL.

After calculating the amount of cells per mL, the project team determined the amount of cells needed per cell concentration. The concentrations were varied to determine which concentration of cells best fit the optimal spheroid size of between 250-500 μm. The project team experimented with cell concentrations of 1,000, 2,500, and 5,000, cells per 40-50 μL drop. These concentrations and volumes were critical when plating hanging drops because if the spheroid is too heavy it could fall from the plate. Similarly, the volumes of each drop/well were critical for the 24 and 96 well plates because if there was not enough media present to cover the entire bottom of the well, the cells could dry out. The calculations completed to determine the cell/media ratio to dilute the cells for plating are shown in Tables 8 and 9.

Table 8. Calculations for 1,000 cells for a 200 µL 24 well plate

Calculation	Description
1 mL = 1000µL / 200µL = 5	To determine the concentration of cells per mL, one mL was divided by the volume of the plate.
1,000 cells per well (5 per mL) = 5,000 cells/mL	The number of cells desired per well was multiplied by the number of wells per mL to determine C_2
C_1 = 15,925,000/mL C_2 = 5,000 cells/mL 15,925,000 / 5,000 = 3,185x dilution	C_1 was divided by C_2 to determine the dilution needed.
Need 24 wells → Make enough for 30 wells 30 wells(200µL per well) = 6,000µL total volume	Calculated the total volume needed by multiplying the number of wells needed (plus a few extra just to be safe) by the volume of each well.
6,000µL total /3,185x = 1.88 µL ratio **Place 1.88 µL of C_1 in 5,998.12 µL media**	Divided the total volume by the dilution to determine the volume ratio. The volume ratio is the amount of C_1 to place in media, which has a volume of the total volume minus the volume ratio.

Table 9. Calculations for 5,000 cells for a 200 µL 24 well plate

Calculation	Description
1 mL = 1000µL / 200µL = 5 mL	To determine the concentration of cells per mL, one mL was divided by the volume of the plate.
5,000 cells per well (5 per mL) = 25,000 cells/mL	The number of cells desired per well was multiplied by the number of wells per mL to determine C_2
C_1 = 15,925,000/mL C_2 = 25,000 cells/mL 15,925,000 / 25,000 = 637x dilution	C_1 was divided by C_2 to determine the dilution needed.
Need 24 wells → Make enough for 30 wells 30 wells(200µL per well) = 6,000µL total volume	Calculated the total volume needed by multiplying the number of wells needed (plus a few extra just to be safe) by the volume of each well.
6,000µL total /637x = 9.42 µL ratio **Place 9.42 µL of C_1 in 5,990.58 µL media**	Divided the total volume by the dilution to determine the volume ratio. The volume ratio is the amount of C_1 to place in media, which has a volume of the total volume minus the volume ratio.

The same calculations were performed for any type of plate that was used, with varying volumes of the well or drop.

Preliminarily experimenting with the cell concentrations and volumes helped determine which concentrations and volumes would be best suited for the team's designs. Knowing the optimal amount of volume and cells needed for our spheroid creations will prevent the team from future deficits in our design validations.

5.0 Design Verification

5.1 Spheroid Formation

For the team to generate results such as spheroid diameter and sphericity, it was important to determine which cells were considered to have successfully formed spheroids. As a result, the project team developed a system to analyze each spheroid and place it into one of six categories. Cells given values ranging from 1-2 were considered compact enough to further analyze. Cells given values ranging from 3-6 were discarded and recorded as not forming spheroids. The characterization of spheroids is described in Table 10.

Table 10. Ranking system to determine which cells formed spheroids for further analysis

Ranking	Description	Example
1	Round and very compact	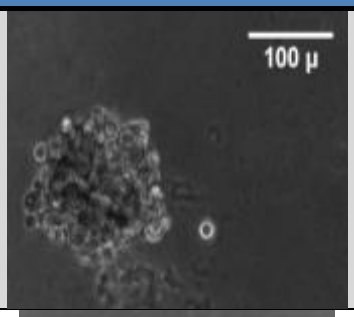
2	Odd/long and very compact	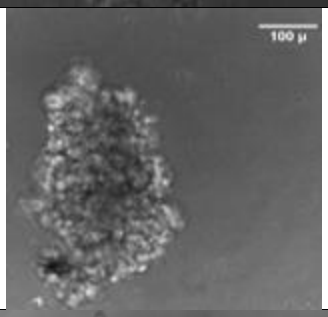
3	Relatively compact with multiple appendages	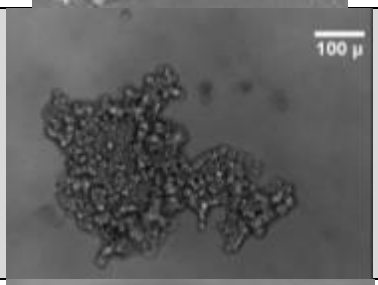
4	Multiple appendages with holes in the body	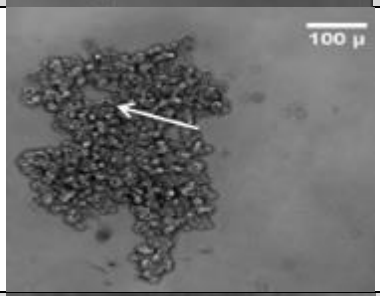
5	Very spread out	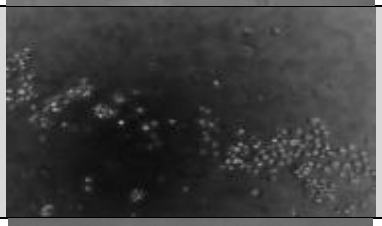
6	No cells / drop fell / bacteria infected cells	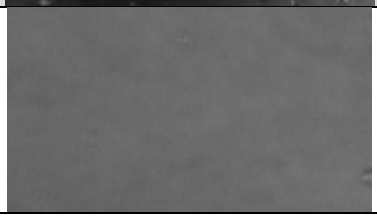

Together the team ranked each spheroid using the ranking system shown in Table 10. The team analyzed the relationship between the number of spheroids formed vs. the plate used to generate them as shown in Figures 15 and 16, where both day 4 and day 7 spheroids are graphed.

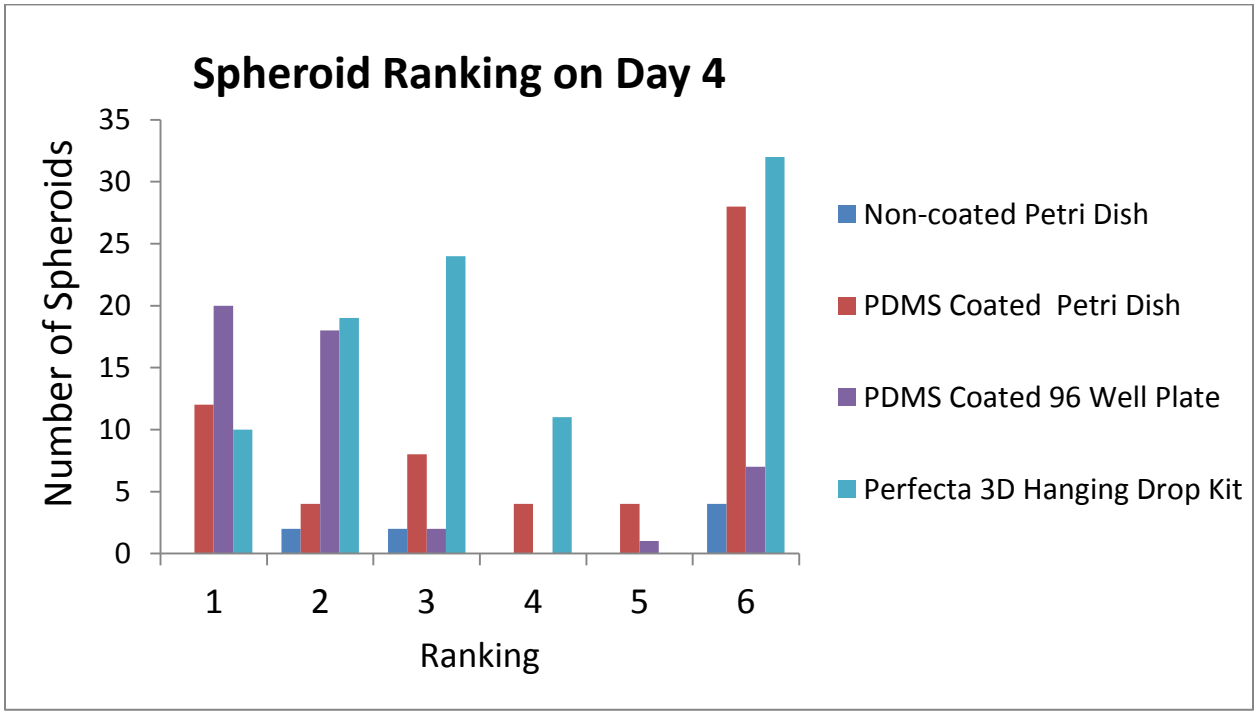

Figure 15. Spheroid rankings on day 4

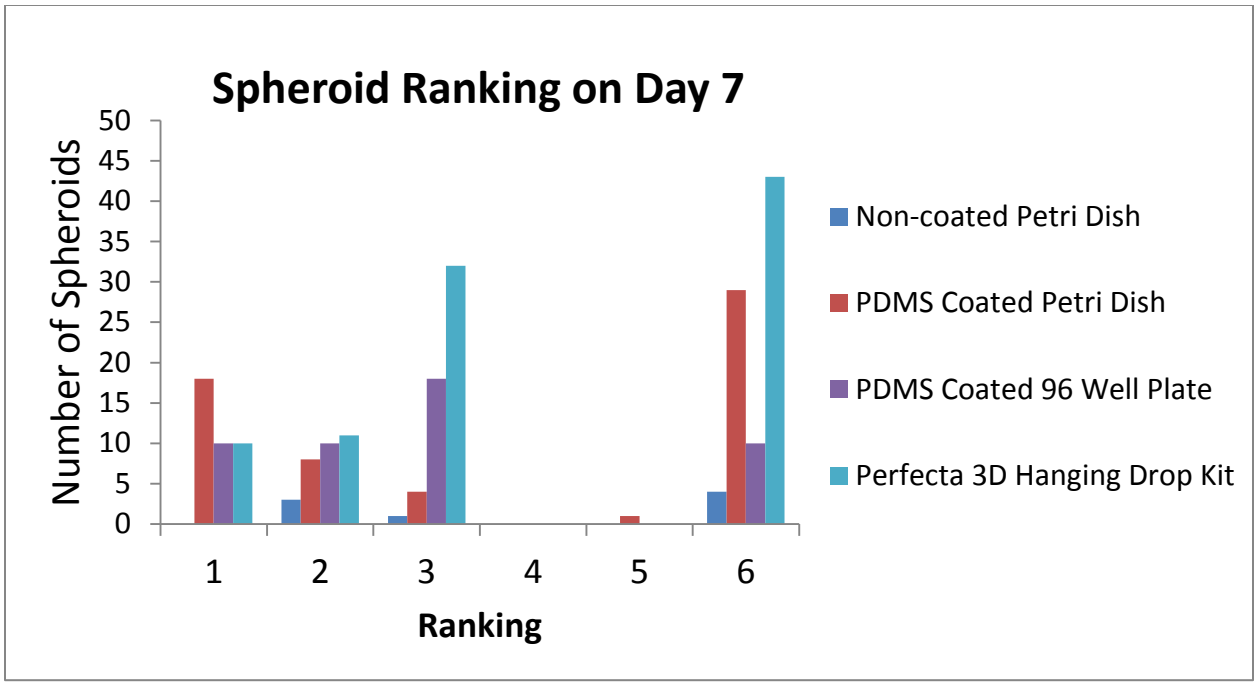

Figure 16. Spheroid rankings on day 7

Since not every device plated the same exact number of spheroids at the beginning, each one was averaged for both day 4 and day 7 as shown in Figure 17.

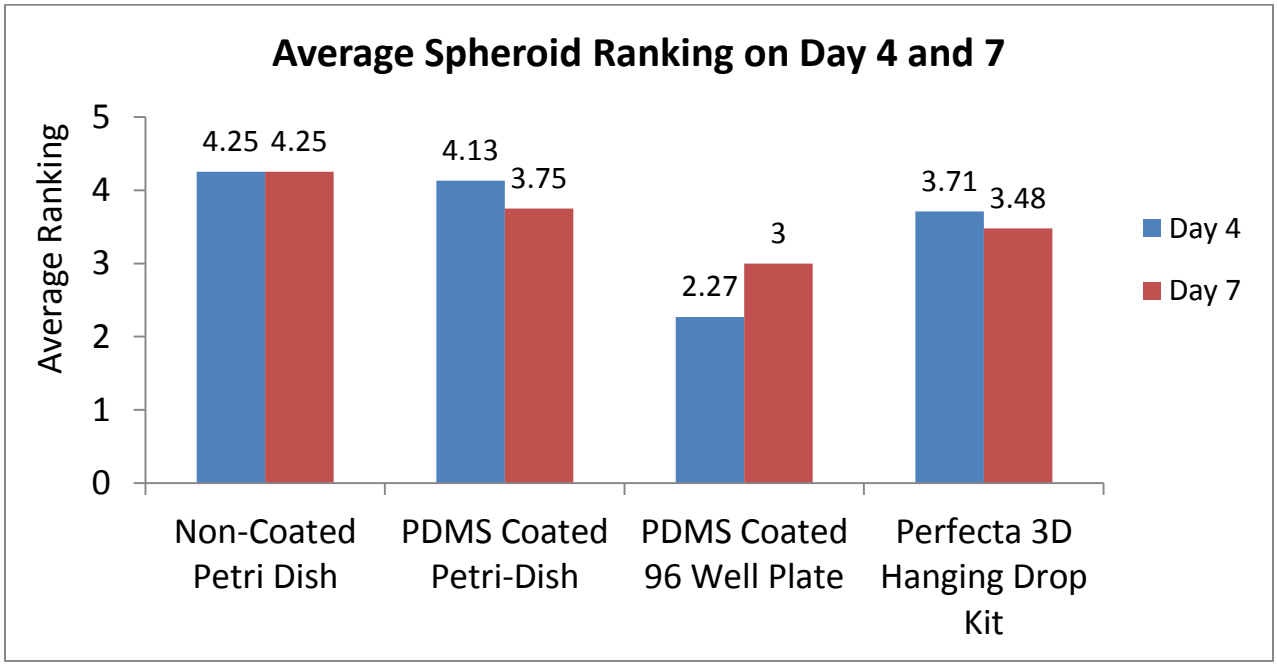

Figure 17. Average spheroid rankings on day 4

5.2 Spheroid Timeline

Spheroids were plated in each cell suspension platform and allowed to grow for 7 days. The cells were imaged on days 1, 2, 3, 4 and 7. A timeline for a spheroid from each device can be viewed in Figures 18-21.

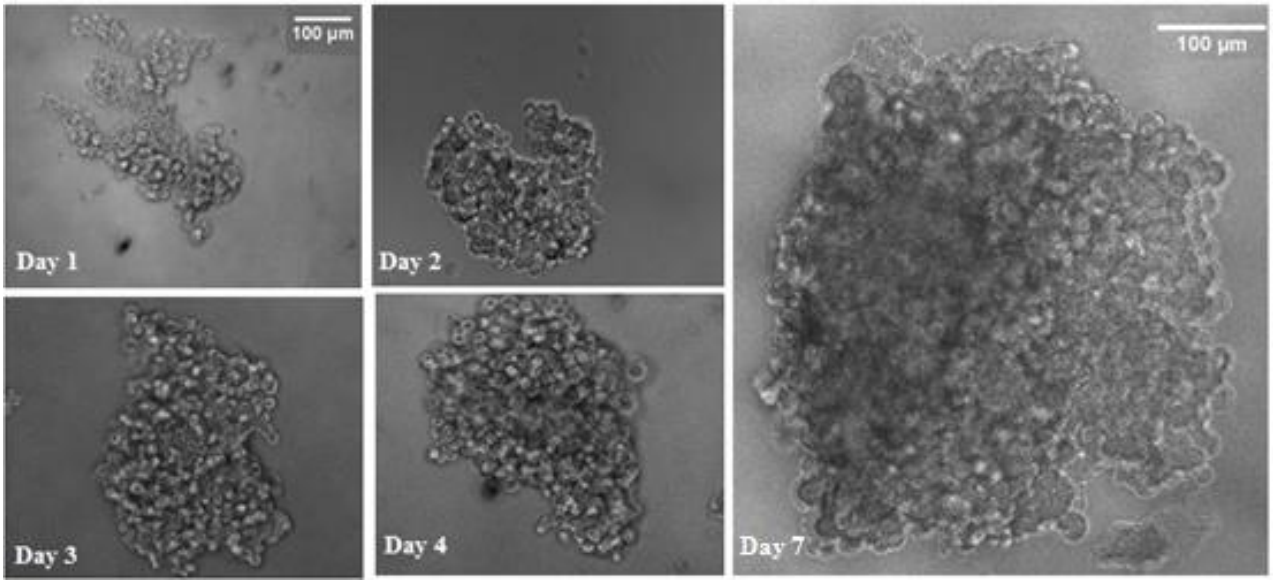

Figure 18. Perfecta 3D Hanging Drop Plate spheroid imaged from days 1 to 7

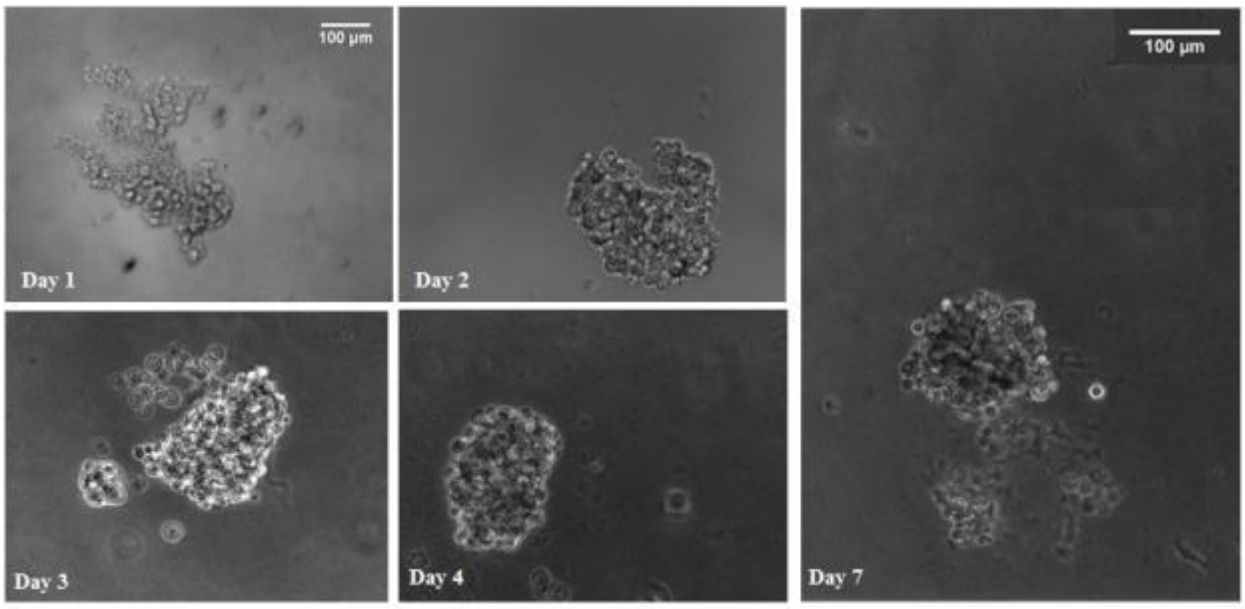

Figure 19. PDMS-coated 96 well plate spheroid imaged from days 1 to 7

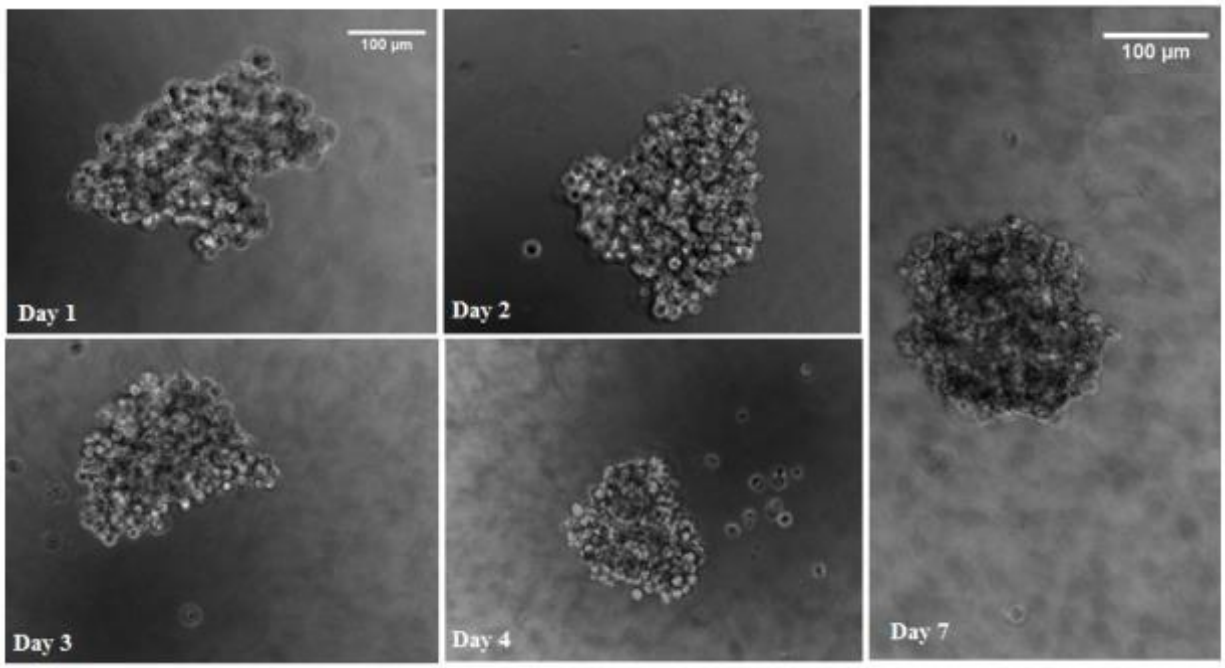

Figure 20. PDMS-coated petri dishes spheroid imaged from days 1 to 7

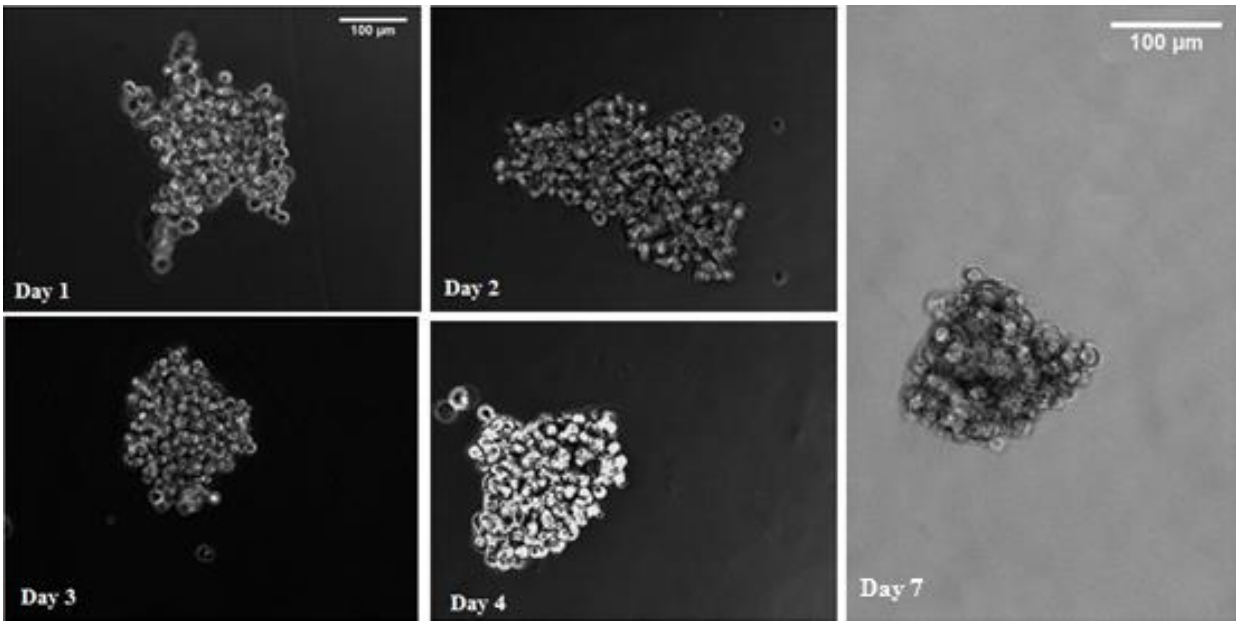

Figure 21. Non-coated petri dish spheroid imaged from days 1 to 7

5.3 Confocal Microscope

Spheroids were transferred from each design alternative into a 96 well plate. The spheroid nuclei were labeled using Hoechst dye 33342 (dilution, 1:500, Molecular probes, Life Technologies). Membrane *in vivo* labeling was obtained with wheat germ agglutinin (WGA) conjugated with AlexaFuor594 flurorphore (dilution 1:500, Molecular probes, Life Technologies). The dyes were added directly to the medium and incubated at 37ºC for 10 minutes. Excess of dyes was washed with PBS and fixed in paraformaldehyde 4% in phosphate buffer for 10 minutes at room temperature. Spheroids were mounted on glass and fluoro-bleaching was protected with a drop of Vectashield (Vector laboratories). After fixation, spheroids were transferred from the 96-well plate by gently pipetting the spheroid with a truncated pipette tip and mounted to a glass slide for confocal imaging (Leica TCS SP5 microscope) using a 405 nm diode laser and 594 nm Ar-He, Ne laser line.

Confocal images were taken to validate cellular morphology in spheroids using blue Hoechst dye 33342 to show the nuclei of Mn9D cells and a WGA stain to visualize cell membranes. Multiple cell layer 3D constructs were captured with Z-stack option, and pinhole of 1 in 1mm steps using Leica confocal software as shown in Figure 22. A complete view of the spheroid is observed in Figure 23.

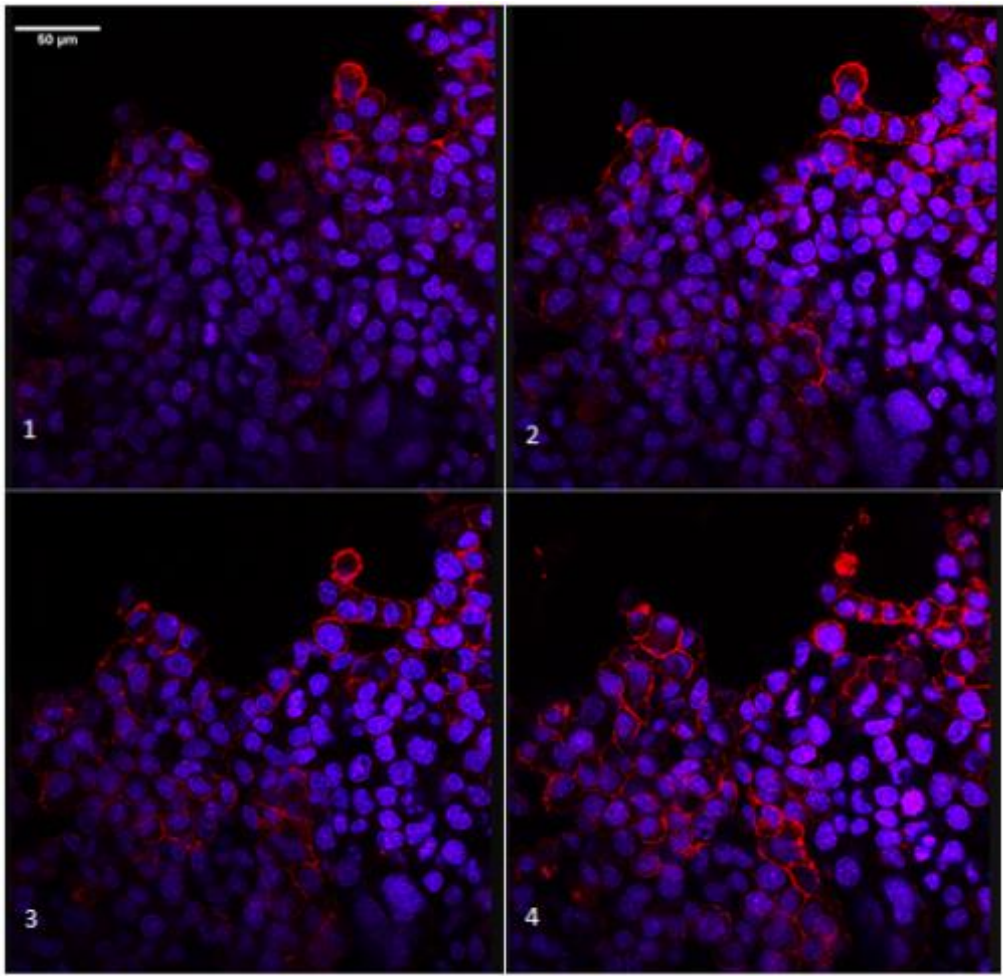

Figure 22.Confocal images of a Mn9D spheroid transferred from a PDMS-coated 96 well plate. 1-4 show various focal planes of cells stained with Hoeschst dye 3342 (blue) and WGA (red).

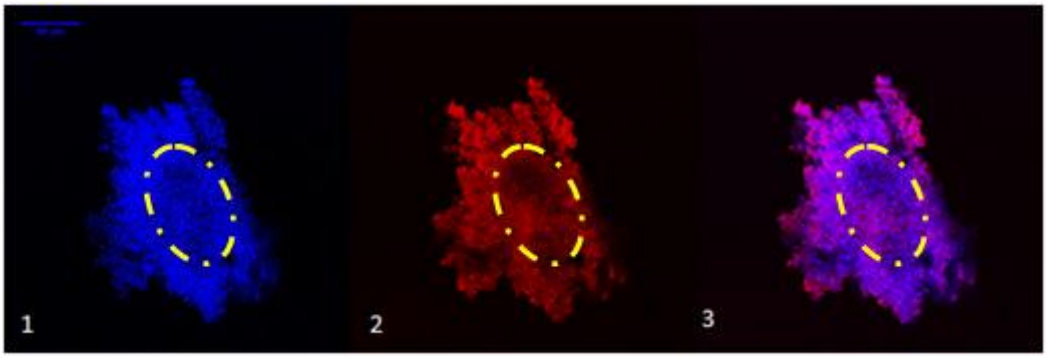

Figure 23. Complete view of a single spheroid transferred from a PDMS-coated 96 well plate. (1) Hoeschst dye3342 stain. (2) WGA stain. (3) Merged image of blue and red channels. Yellow regions indicate a less dense center.

5.4 Spheroid Functionality

To determine if the spheroids would serve as a functional and physiologically relevant model for neurodegeneration and cytotoxicity screening, the project team used DAPI stained samples and MTT assays on 3D models. Results were compared to 2D data to determine similarities.

5.4.1 DAPI staining

DAPI stains were added to wells with spheroids and imaged to show that the aggregates seen under the microscope were in fact aggregates of cells and not debris or artifacts from plate coatings. The protocol for DAPI staining can be found in Appendix Q. DAPI stained samples comparing 2D and 3D cells are shown in Table 11.

Table 11. Phase images on the left of 2D (top) and 3D (bottom) and images of DAPI-stained samples images on the right

Cell Type	Phase	DAPI
2D	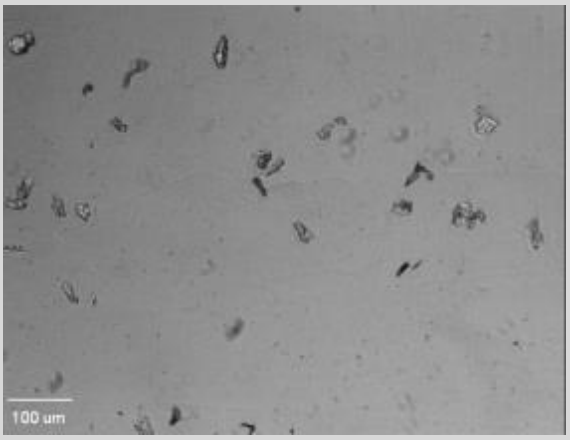	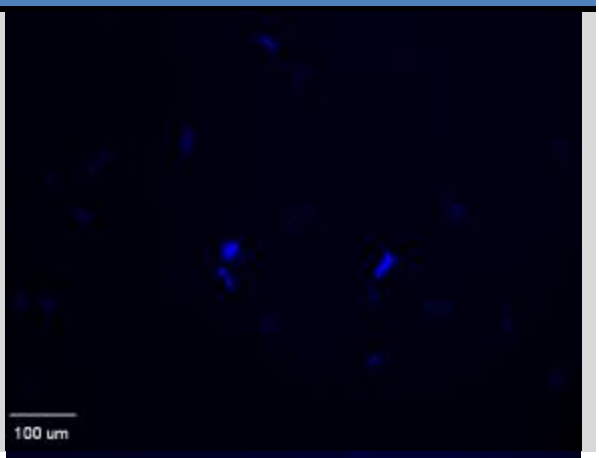
3D	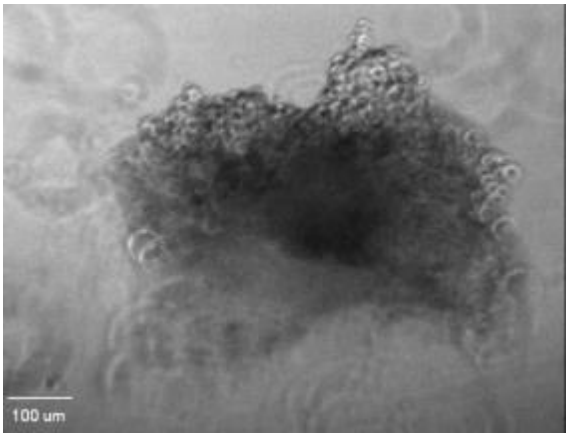	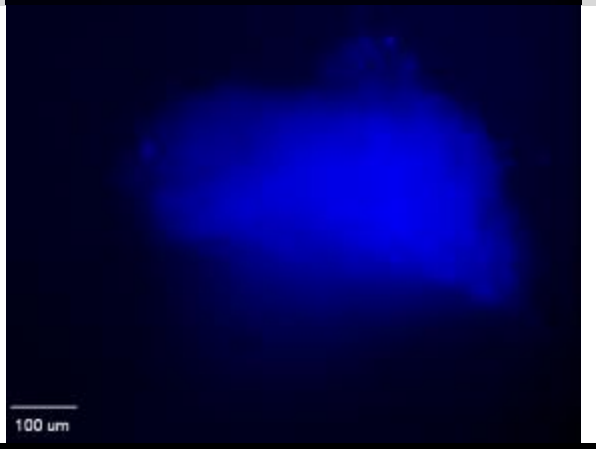

5.4.2 MTT Assay

The project team performed several MTT assays to assess the toxicity of each pesticide on the cells grown in 2D, on the hanging drop plate, and in the PDMS-coated 96 well plate. MTT assays are used to quantify cell viability based on a healthy cell's enzyme that breaks down the dye and produces a purple color. Therefore, wells with healthy cells turn dark purple and wells containing dead cells will have little purple color as shown in Figure 24.

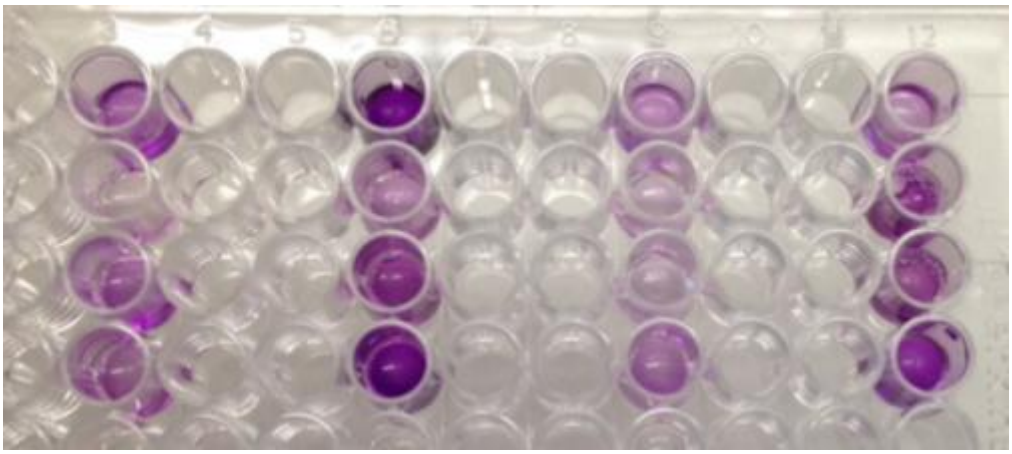

Figure 24: MTT assay color change. An example of 3D spheroids with more purple color indicates increased metabolic activity.

The protocol used by the project team to perform MTT assays is described in Appendix R. The project team only had successful MTT assays on cells grown in 2D, in the Perfecta Hanging Drop Plate, and in the PDMS-coated 96 well plate. The results of the MTT assays on Mn9D cells with a concentration of 5,000 cells per well/drop exposed to 10μM of pesticides (Rotenone, Confidor, and IMI) and a control of cells with just media are shown in Figure 25.

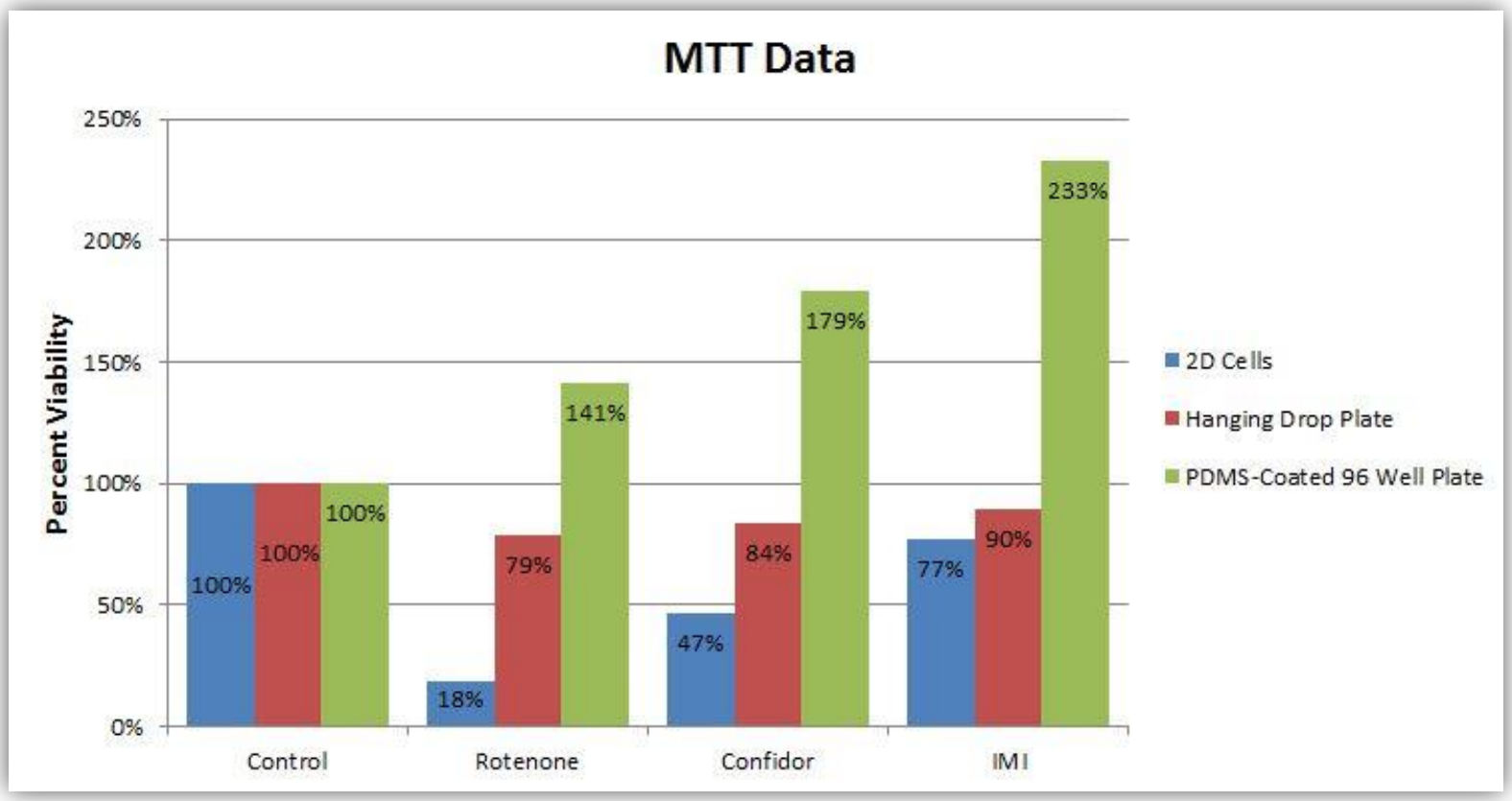

Figure 25: MTT data where n=1 for each cell suspension platform

5.5 Ideal Spheroid Concentration

An important objective was creating spheroids that were consistent in shape and size. In particular, the cell concentration chosen should create spheroids with diameters between 250-500 µm. If spheroids have diameters larger than 500 µm they risk the chance of forming necrotic core (Vinci, 2012). The best way to manipulate spheroid size is by adjusting the concentration of the supernatant as described in Section 4.4 Experimental Methods. Diameters of spheroids were measured using ImageJ and averages were calculated (Appendix S).

Experiments were originally set up using conventional hanging drop methods and PDMS-coated petri dish tops. Cell concentrations were calculated as described in Section 4.4.1 Cell Culture and Spheroid Formation and then the drops were pipetted onto the cover of a petri

dish. Some of the covers were coated with a thin layer of PDMS. Because PDMS is a hydrophobic material, the drops on this surface had higher contact angles than the non-coated petri dish cover (Guilhem, 2013). The higher contact angles created a more spherical drop, which allowed the cells inside the drop to take on a similarly spherical shape. Also, the PDMS-coating gave the drops more structure, which increased the drops' integrity during the process of carefully flipping the petri dishes over and placing them on the bottom petri dishes so the cells could hang down. Figure 26 compares the very spherical drops on the PDMS-coated petri dish and ruined drops on a non-coated petri dish after flipping.

Figure 26. PDMS-coated petri dish on the left vs. non-coated petri dish on the right

In addition to testing hydrophobic surfaces, the project team also experimented with number of cells per drop. Cell concentrations of 1,000, 2,500, and 5,000 cells were placed in 40µL of media to determine which concentration formed the most compact spheroid with diameters less than 400µm. Cells were imaged daily to check for aggregation and cell proliferation. A downfall to the hanging drop methods is that media can't be added or changed daily without disturbing the drop and risking it falling. As a result, approximately 2mL of PBS was placed in the bottom of the dishes to keep the drops from drying out.

Table 12. Comparison of spheroid diameters from plating of concentrations of 1000, 2500, and 5000 cell supernatants. Each was plated as either a conventional hanging drop or on a PDMS-coated petri dish cover

Device	Image	Cell Concentration and Volume of Media	Average Cell Diameter (µm)
Non-Coated Petri Dish	Not enough form spheroids to get accurate data (1/16)	1000 cells/40 µL	N/A
	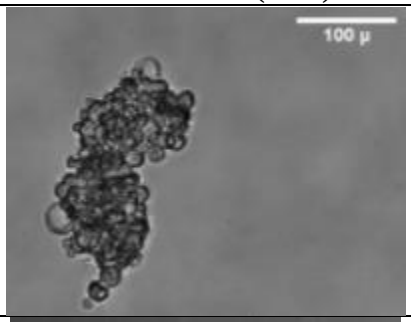	2500 cells/40 µL	212.69
	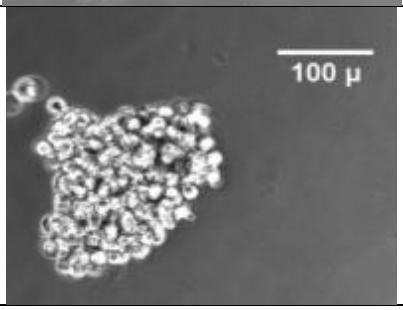	5000 cells/40 µL	280
PDMS Coated Petri Dishes	Not enough form spheroids to get accurate data (2/16)	1000 cells/40 µL	N/A
	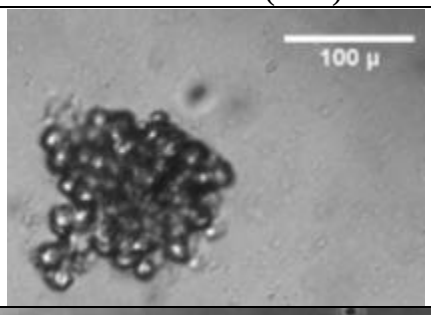	2500 cells/200 µL	268
	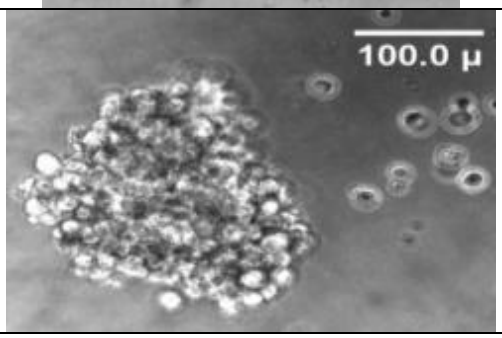	5000 cells/40 µL	396

By day four, the cells formed clusters seen in Table 12. The diameter of each cluster was measured and recorded. The cells were returned to the incubator to continue growing for a couple days longer, however the project team found there wasn't much change after day 4, so the team decided to try other methods that might give better results.

5.6 Ideal Spheroid Forming Device

5.6.1 Diameters

As mentioned above, the team found it necessary to create spheroids between 250- 500 µm (Vinci, 2012). After adjusting the concentrations and settling on a concentration of 5,000 cells per spheroid, the team tested this concentration in varying devices. The devices chosen from the design alternatives to compare were – a conventional hanging drop, PDMS-coated petri dish covers, a PDMS-coated 96 well plate, an agarose coated 24-well plate, shrinky-dinks, and the 3D printed molds. A non-coated 96 well plate was used as a control to compare with the PDMS- and agarose-coated ones. The average diameters of spheroid created after 4 and 7 days in each device are shown in Figure 27. Only spheroids receiving a rank of 1 or 2 from Table 18 were included in the calculation, which were made using ImageJ and Excel.

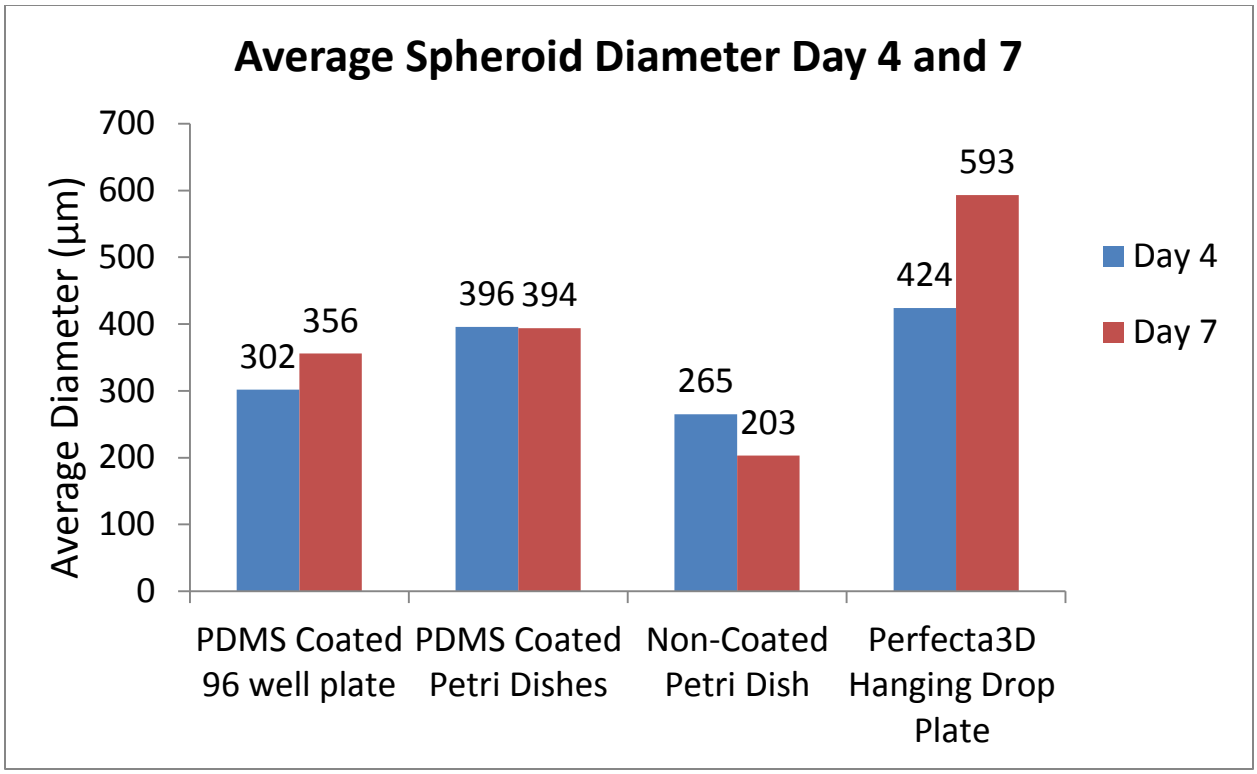

Figure 27. Average spheroid diameters for each device on day 4 and day 7

5.6.2 Sphericity

The sphericity of each spheroid was calculated to provide data about the compactness and quality of the microtissues formed. The sphericity was calculated using the following equation of H. Waddell's ellipsoid-based sphericity formula sphericity (Lee et al., 2009):

$$\Psi\ (sphericity) = \frac{2\sqrt[3]{ab^2}}{a+\frac{b^2}{\sqrt{a^2+b^2}}*\ln\left(\frac{a+\sqrt{a^2-b^2}}{b}\right)} \qquad (1)$$

where *a* represents the semi-major axis and *b* represents the semi-minor axis. Semi-major and –minor axes were calculated using Eq. (2) and (3) respectively as shown in Figure 28, where f_1 and f_2 are the focal points and F is the distance between the focal points. These areas are

indicated on a Mn9D spheroid created by the design team using a PDMS-coated 96 well plate in Figure 29 and measured using ImageJ software.

Semi major axis (a) = ½ (A+B) (2)

Semi minor axis (b) = ½ $\sqrt{(A+B)^2 - F^2}$ (3)

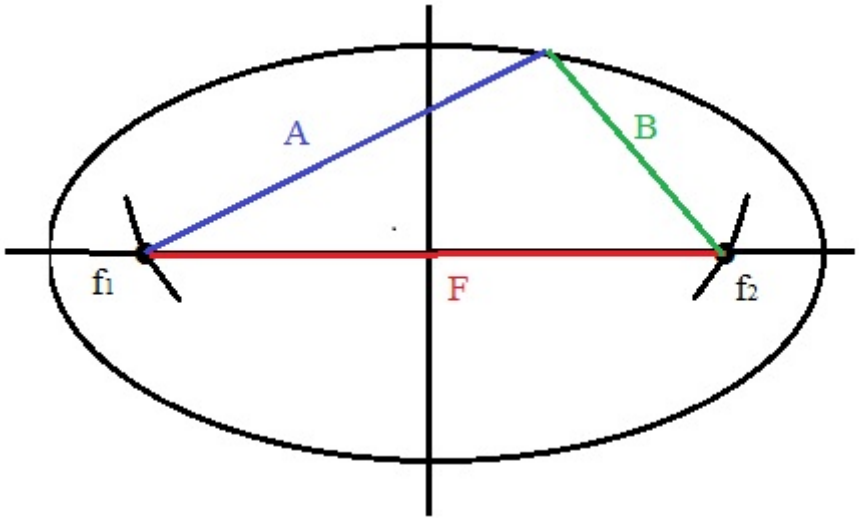

Figure 28. Drawing of an ellipse showing the points used to calculate the semi-major axis and semi-minor axis.

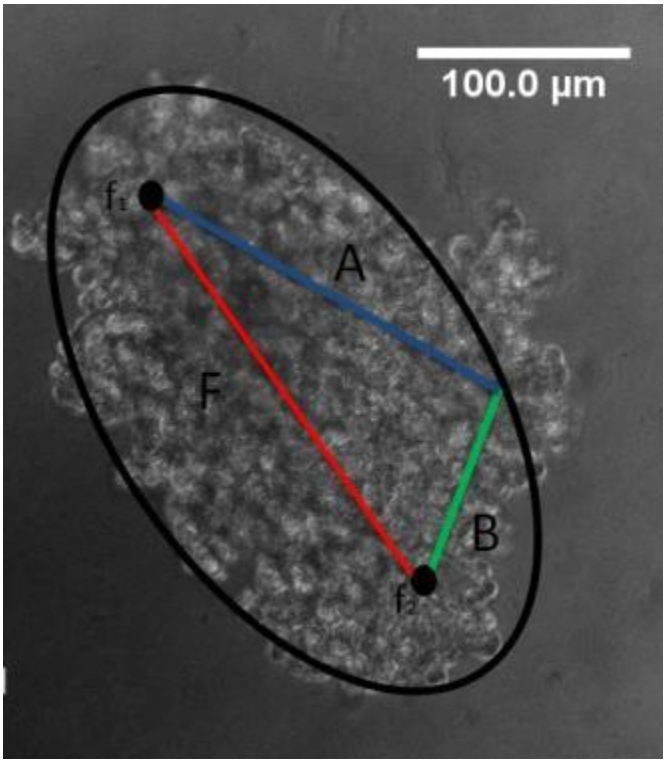

Figure 29. Schematic of semi-major (a) and semi-minor axis marked on a MN9D cell of a PDMS-coated 96 well plate

The team used H. Waddell's sphericity equation on all working prototypes of hanging drop plate designs to determine which design formed the highest degree of sphericity for Mn9D spheroids. A value of Ψ=1 indicates a high degree of sphericity (Lee et al., 2009; Cavarretta, et al., 2009). Results for average sphericity are shown in Figure 30.

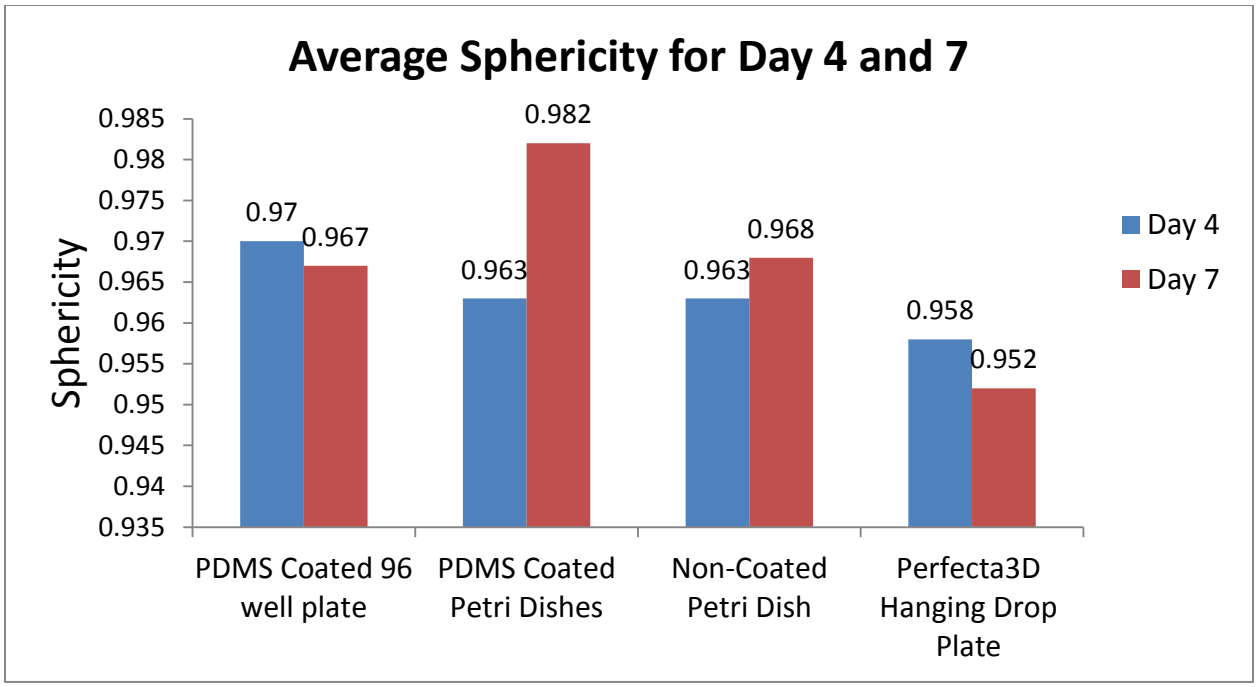

Figure 30: Average sphericity of each designed prototype for creating spheroids.

5.7 Plating Efficiency

After experimenting with different concentrations to use when forming spheroids and ruling out devices that were unable to form spheroids, the team looked to analyze the effectiveness of each device. Figure 31 below shows the percent of spheroids formed from each device and Table 13 lists the number of cells plated for each design alternative.

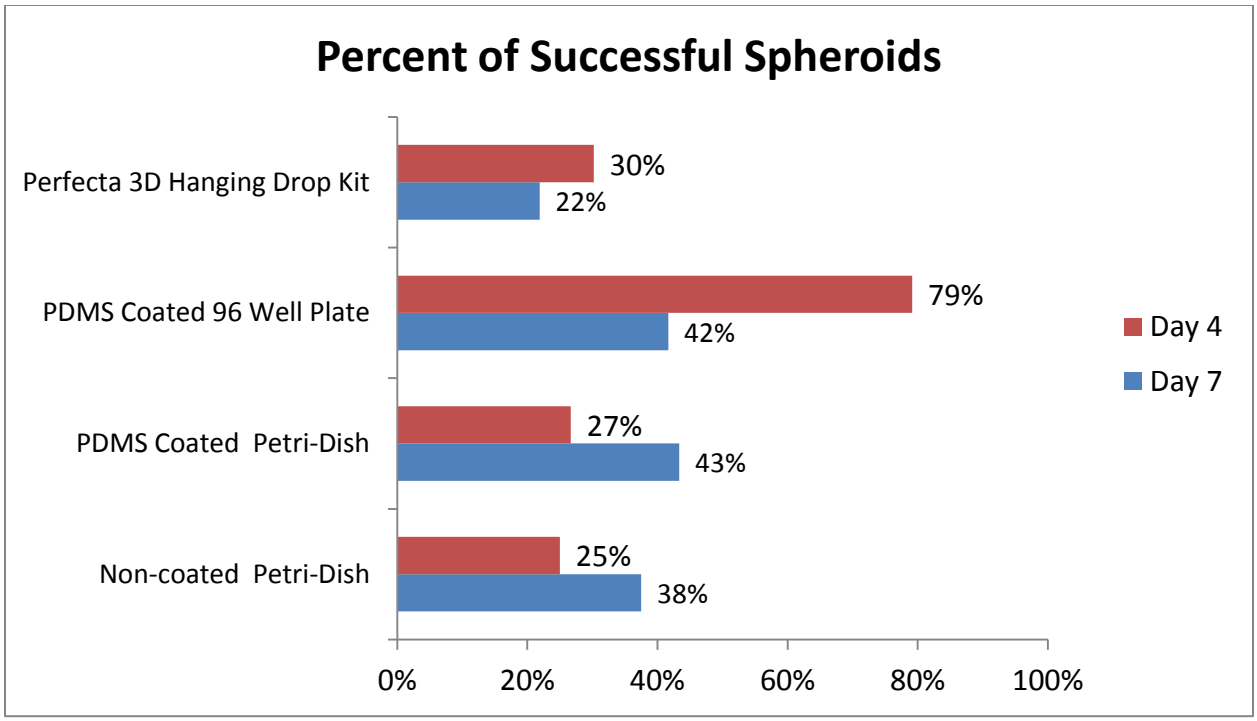

Figure 31. Percent of spheroids formed based upon rankings by day 4 and 7

Table 13. Number of cells plated for each design alternative

Device	Cells Plated
Perfect 3D Hanging Drop Kit	96
PDMS-Coated 96 Well Plate	48
PDMS-Coated Hanging Drop Petri Dish	60
Non-coated Hanging Drop Petri Dish	8

Another important consideration of the design is the price it would cost to create each spheroid. This can be calculated using the percentages in Figure 31 above. Multiplying the success rate of each device by the number of spheroids plated allows a predicted spheroid output to be calculated. Dividing the spheroid output by the total price of the device used to plate the

spheroids allows one to calculate the price/spheroid of the device chosen. Table 14 shows hypothetical results of the cost to plate 96 spheroids for each design alternative.

Table 14. Price to plate 96 spheroids for each design alternative

Device	Price	# Needed	Total Price	Success Rate by Day 4	Predicted Spheroid Output	Price/Spheroid
PDMS Coated 96 Well Plate	$2.07 per plate	1	$2.07	79%	75.84	$0.03*
PDMS Coated Petri Dish	$0.40 per plate	24	$9.60	27%	25.92	$0.37*
Non-Coated Petri Dish	$0.40 per plate	24	$9.60	25%	24	$0.40
Perfecta3D Hanging Drop Plate	$25.75 per plate	1	$25.75	30%	28.8	$0.89

* PDMS coated plates would be a bit more expensive because of the cost of PDMS ranges from $0.12-$0.17 per gram

6.0 Discussion

6.1 Spheroid Formation

The PDMS-coated 96 well plate and the Perfecta3D hanging drop plate formed the most compact spheroids with rankings of either a 1 or 2, as shown in Figure 15 and 16. The PDMS-coated 96 well plate formed a total of 38 spheroids on day 4 and 20 by day 7 (in 48 wells), whereas the Perfecta3D hanging drop kit formed 29 spheroids on day 4 and 21 on day 7 (in 96 wells). To take into account the differences in number of spheroids plated, an average ranking was calculated for each plate. Again, the PDMS-coated 96 well plate had the highest rankings, followed by the PDMS coated petri dish.

The team also noted the differences between day 4 and day 7. On day 7, the team decided to go back and once again rank each spheroid. They found that many spheroids that had once been ranked as 1's, were now being ranked as 3's. This appeared to be a result of the formation of small appendages that had formed while the spheroids sat over the weekend. The team believes this is because the spheroids started to become too large. As a result, the project team decided it was better to perform testing on the spheroids after 4 days rather than 7.

6.2 Spheroid Timeline

The team observed an increase in the spheroid compactness in each design alternative over a 7 day period. On day 1, most spheroids were more scattered in appearance and showed limited compactness and rounded shape. Then, by day 7, the spheroids had acquired a more rounded shape. The spheroids became a bit darker in color indicating more compactness and the building of cell layers creating the 3D spheroid structure.

6.3 Confocal Microscope

Spheroids were validated with confocal imaging by capturing spheroids of 28 to 64 micron thick structures. Figure 32 displays stained nuclei, confirming the observed structures were Mn9D cells, and bright red borders show cell to cell interaction between cells of the spheroid (28 µm thick, 3 µm thick sections, 1.7 zoom). The shared borders of cells in the spheroid prove compactness of the cells within the spheroid. Spheroid compactness was also validated by the strength of signal displayed by the brightness of the fluorescence viewed in the complete spheroid (Figure 23 above). Figure 33 displays a process of Mn9D cells inside the spheroid showing the potential for cells to differentiate and function as a physiological model for Parkinson's Disease.

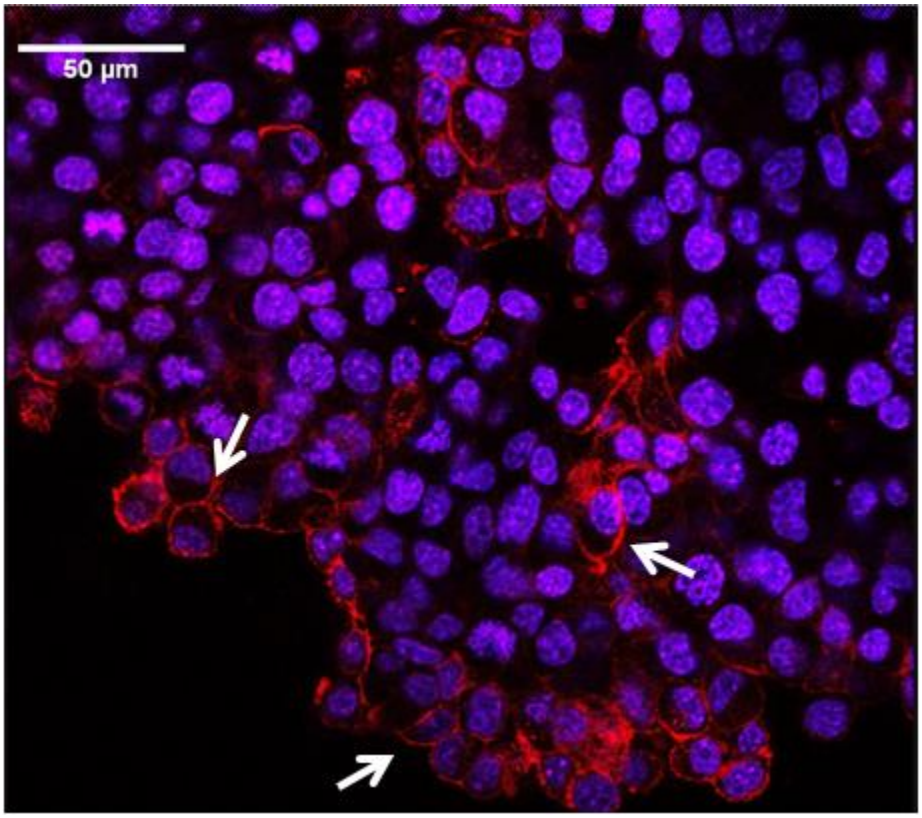

Figure 32. Confocal images of a MN9D spheroid transferred from a PDMS-coated 96 well plate. White arrows indicate areas of membrane interaction.

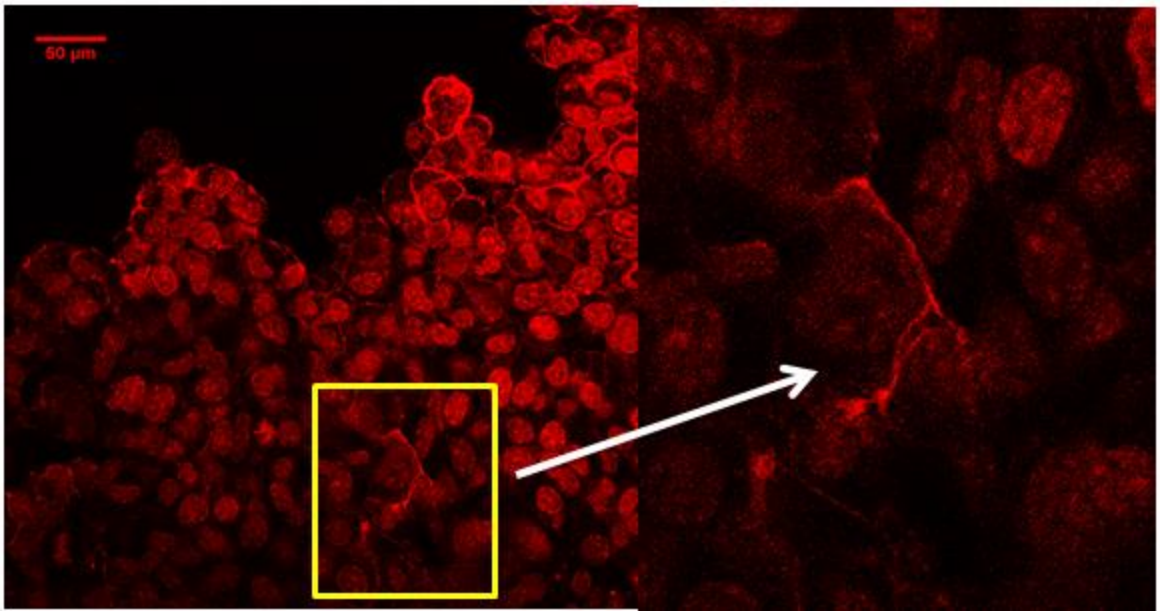

Figure 33. Confocal images of a MN9D spheroid transferred from a PDMS-coated 96 well plate. The yellow box highlights a process of a MN9D cell. The white arrow indicates an enlarged perspective.

Spheroids that have a thicker structure (over 60 µm) were observed to have gaps in the center. When a spheroid is too thick, one possibility is that it can prevent the profusion of dyes and stains to the center, inhibiting the staining of nuclei and cell borders or prevent the profusion of fresh media to the center, leading to cell death. Gaps may also be a resulted of bleached flurophores from overexposure to normal light. Figure 34 displays the necrotic core/gaps of a 64 µm spheroid with 7 µm layers capture with 40x magnification.

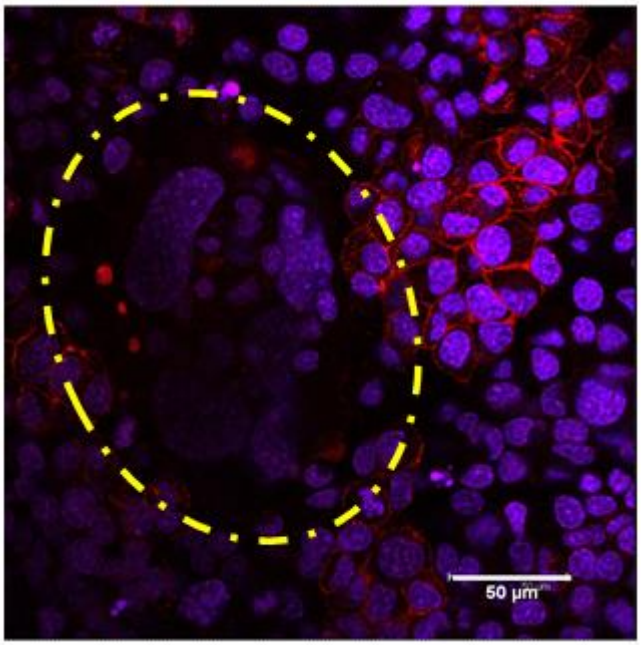

Figure 34. Mn9D spheroid transferred from the PDMS-coated 96 well plate. The region circled in yellow indicates the gaps/necrotic core of the spheroid.

6.4 Spheroid Functionality

6.4.1 DAPI Staining

On the first attempt at DAPI staining the spheroids, the project team found very little fluorescence. The project team believes that the compactness of the spheroid limits the ability of the DAPI stain to penetrate into the center of the spheroids in the short 10 minute exposure time, so, without fixing the cells, the spheroids were left in the DAPI stain overnight. The images acquired the next day were showed much more fluorescence. The amount of fluorescence is almost too much because there are 5,000 cells in multiple layers being illuminated at once. The comparison of the DAPI stained 2D cells to the 3D spheroids verified that the groupings in each cell culture were in fact cells. Furthermore, the DAPI staining verified the number of cells and their compactness in the spheroids.

6.4.2 MTT Assay

The project team expected to obtain MTT results where the control had a viability of 100% and the pesticides had increasing viabilities in the following order: Rotenone, Confidor, and IMI. The results shown in Figure 25 demonstrate the same trend that the project group expected to see. However, there were a few limitations to this data. First, the PDMS-coated 96 well plate has much higher cell viability values for the pesticides than the control. This cannot be true because the pesticides should cause some cell death, while the control cells were only exposed to media, thus should be healthy. The project team believes there was some human error that killed the cells in the control group. Second, the cell viability values for the spheroids follow the same trends as the 2D cells, however, the overall percent viabilities are much higher in the 3D cultures. The project team believes this is due to the compact structure of the spheroids, which makes it much harder for the pesticide to penetrate into in the 16 hour exposure time. If the spheroids were exposed to the pesticides for a longer amount of time, it is reasonable to believe that the percent viability values would be closer to those of the 2D cells.

6.5 Ideal Spheroid Concentration

Table 12 shows that supernatants containing 1,000 cells/40 µL were unable to create enough spheroids to get significant data. As a result 1,000 cells were quickly discarded as a spheroid concentration. 2,500 cells/40 µL created spheroids with diameters averaging of 212.69 µm in non-coated petri dishes and 268 µm in PDMS coated petri dishes. 5,000 cells/40 µL created spheroids that averaged 280 µm for the non-coated petri dishes and 268 for the PDMS-coated petri dishes after 4 days. This fell right in the range of 250 – 400 µm. As a result, the project team selected a concentration of 5,000 cells for the final design.

6.6 Ideal Spheroid Forming Device

6.6.1 Diameters

Figure 27 compares each device with the average diameters of the spheroids it formed on day 4 and day 7. The PDMS-coated 96 well plate had spheroid average diameters falling right in the middle of 250 and 500 µm on both day 4 and day 7. The team took note that on day 4 there were more spheroids produced and more spheroids falling into this range. The Perfecta3D hanging drop plate had an average spheroid diameter of 424 µm by day 4, however the spheroids continued to grow drastically into day 7 and surpassed 500 µm. As a result there is strong

The petri dishes both had spheroid diameters falling in between the desired range of 250 and 500 µm on day 7. The non-coated petri dish had one that was slightly lower on day 4 averaging around 203 µm. The team predicted that this had to do with the evaporation of media from the drops. Even with the PBS in the bottom of the dish to prevent evaporation, the size of the media drops were smaller each day as they began drying out. This is the most plausible reason as to why the diameters of the spheroids plated in the non-coated petri dish shrunk from day 4 to day 7.

6.6.2 Sphericity

The PDMS-coated 96 well plate had the highest average sphericity of all the design alternatives by day 4 (.97). However, by day 7 the PDMS coated petri-dishes had the highest with an average of .982 followed by the non-coated petri dish averaging .968. Both days the Perfecta 3D hanging drop plate had the lowest sphericity of all 4 design alternatives. Though it's important to note that overall PDMS coated petri dishes scored the highest, their success rate in forming spheroids is much lower than PDMS coated 96 well plates (79% vs. 27%).

6.7 Plating Efficiency

Figure 31 is important in visualizing the effectiveness of each plate in creating spheroids. The PDMS-coated 96 well plate with a 79% success rate on day 4 was the only design alternative to achieve a score over 50%. The non-coated petri dish and PDMS-coated petri dishes had the worst success rates of only 25% and 27% respectively. These low scores are due to many of the drops drying out and/or falling. Hanging drops are very fragile, which makes imaging without disturbing them difficult. There is also no way to change the media, so many of the drops dry out while sitting in the incubator.

The Perfecta3D hanging drop plate surprised the team with its highest success rate at 30% on day 4. This was due to the drops falling or forming spheroids that fell into a category between 3-5. Though more stable than the petri dishes, the hanging drop plate still has the potential for drops falling if moved too quickly. The team lost all of row H when the plate was moved too quickly and the distilled water in the reservoir spilled onto the row. By day 7, the team found that most of the drops had formed large appendages that made it hard to calculate sphericity, which made it difficult to classify the drops as spheroids.

The PDMS-coated 96 well plate is effective because its drops are less fragile than the other design alternatives. The cells are durable because they are at the bottom of the well, so slight disturbances to the plate do not destroy the spheroids. This design also allows for easy exchange and addition of media. Media can be carefully taken off/added to the top of each well when needed, keeping the cells fully hydrated. This design alternative is much more high throughput than the petri dishes because 96 wells can be plated, whereas the petri dishes can only hold 4 drops per dish.

The PDMS-coated 96 well plate had the lowest predicted price per spheroid seen in Table 14. Including the price of PDMS, the price averages out to about $0.30 per spheroid. This is less than half the price of the Perfecta3D hanging drop plate and slightly less than the conventional hanging drop formed on non-coated petri dishes.

6.8 Economics

The economic impact of the team's final design of a PDMS-coated 96 well plate would serve as a simple, low cost, and user friendly device for creating a physiologically relevant model to assess neurodegeneration and cytotoxicity. Labs and researchers would be able to steer away from more expensive animal testing. Many lab animals will be saved by reducing the need for animal LD_{50} designed experiments. The team's device also provides a cheaper alternative to expensive, commercialized 3D hanging drop plates that are on the market today. An estimate of the cost of using this design is shown in Table 15.

Table 15. Cost of final design

Materials:	Price
Mn9D Cells:	$0.00
Media:	
FBS (10mL)	$10.00
F-12 Nut Mix (100mL)	$5.00
DMEM (250mL)	$10.00
96-Well Plate:	$2.07
Ethanol (500mL)	$8.00
Pipette Tips	
10uL	$57.00
200uL	$60.00
1000uL	$72.00
Trypsin (5mL)	$1.34
Serological Pipette Tips (15)	$18.00
Falcon Tubes (3)	$1.44
PBS (500mL)	$14.00
Large Petri Dish:	$2.20
G418 (1G)	$35.00
Doxycycline (1G)	$63.30
Pesticides	
Confidor	$1.00
Rotenone	$5.00
IMI	$24.00
Total:	**$389.35**

6.9 Environmental Impact

By providing a new method to conduct cytotoxicity tests with a valid, physiologically relevant model, more tests on pesticides can be conducted without harming animals. Understanding the cytotoxicity of certain pesticides and compounds can provide agencies and business with information regarding the risk of using certain toxins has on the surrounding environment, including humans. Furthermore, the PDMS used for the project team's final design is does not have negative environmental impacts when it degrades. PDMS is converted back to

inorganic ingredients (water vapor, amorphous silica, and carbon dioxide) allowing it to be able to be reused and pose as less of a threat to the environment. There have not been any known harmful effects from PDMS or its degradation products on plant growth and survival, birds, or insects. PDMS fluids also pose no known hazard to the environment. PDMS is not considered a hazardous waste, unlike primary cell cultures from lab animals (Dow Corning, 2012; Auner et al., 2008).

6.10 Societal Influence

Using a PDMS-coated 96 well plate as a means for cytotoxicity screening will eventually help reduce the impact of harmful chemicals and compounds into surrounding areas. Utilizing this high throughput device could lead to the ban of harmful pesticides if enough information can be obtained from using physiologically relevant models. By banning the use of pesticides, humans and animals will have less exposure to the toxins that cause neurodegeneration, thus the occurrence of neurodegenerative disorders may decrease.

6.11 Political Ramifications

The project team's PDMS-coated 96 well plates could influence the global market by providing researchers in international labs the opportunity to move away from animal testing for further research and discovery on neurodegenerative diseases and pesticides. The design provides a way to take an engineered cell line and create a microtissue structure that can mimic physiological mechanisms of an organ or tissue. Mn9D spherioids can be used as a model for Parkinson's Disease, eliminating the need to euthanize many animals around the world. Over time, with enough cumulated research, the data gained by using this design could potentially gain government support to better regulate the use of pesticides in many countries.

6.12 Ethical Concerns

Ethical concerns over the use of animals as scientific models for drug screening have existed for many years. Testing on animals has allowed most drug products to safely enter the market for human use. Animal testing has also played been an important part in the discovery of environmental factors that can cause harm to humans. However, due to the ethical concerns surrounding the use of animals in scientific research, the production of a new approach to replace the use of animals would be most beneficial and welcome in the scientific community. 3D spheroids are just that approach. In particular, Mn9D spheroids could be used in studying Parkinson's Disease and would serve as a more predictive model of human responses to toxins than regular 2D cultures.

6.13 Health and Safety

The project team hopes that Mn9D 3D spheroids will not only play a role in replacing the use of animals in scientific research, but they will also contribute to the continued effort to understand neurodegenerative diseases such as Parkinson's Disease. As representative models of the brain, these spheroids can be used to predict the effects of environmental factors, such as pesticides, on the human brain. A big picture view shows that this research can ultimately influence human healthcare by making sure environmental factors that are dangerous to human health are off the markets and used only in controlled environments.

6.14 Manufacturability

One of the most beneficial aspects of the PDMS-coated 96 well plate is its simple process of manufacturing. The only materials necessary to make the actual design are the PDMS ingredients and a 96 well plate. This design has the potential to be manufactured in a sterile

environment and individually packed to save time and energy of the user having to make the PDMS coatings themselves.

6.15 Sustainability

While there is energy required to make the PDMS-coated 96 well plate, there is no direct energy consumption involved in using the device. Energy is required to solidify the PDMS coatings in the wells in the oven and UV light is required for sterilization. There is further energy needed while the device is used for cell culture, including energy required to run the incubator, the sterile hood, and a microscope for imaging. The project team believes this device is very simple, yet effective for its users.

7.0 Final Design and Validation

The tests performed throughout the short seven weeks for this project helped the project team develop this optimized final design as a system for creating Mn9D spheroids. The project team performed several tests to validate the functionality of the Mn9D spheroids formed using the final design and to verify that the design met the project objectives.

7.1 Final Design

A standard 96 well plate was coated with PDMS to form a hydrophobic surface to promote spheroids formation. The PDMS was created using a 10:1 ratio of silicone elastomer and silicone elastomer curing agent. The two ingredients were mixed until there were no bubbles present. Approximately 200µL of PDMS was pipetted into each well of the 96 well plate. The PDMS-coated 96 well plate was placed in the oven at 80°C for approximately 20 minutes to allow the PDMS to solidify before use. After the PDMS had solidified, the plate was sterilized by filling each well with ethanol and exposing the plate to UV light in a sterile hood for 30 minutes. After sterilization, the wells were aspirated of ethanol and washed three times with PBS.

Once the PDMS-coated 96 well plate was sterilized, the Mn9D cells were split and counted for plating. Mn9D cells were grown in 10% Fetal Bovine Serum (FBS) media. The FBS was filtered using a 0.45µm filter prior to mixing with the other ingredients. The media consisted of 45% DMEM (1x) + GlutaMax, 45% F-12 Nut Mix (1x) + GlutaMax + Penicillin and Streptomycin, and 10% FBS. The media was stored in a 4°C refrigerator and heated in a 37°C water bath prior to use. Similarly, the trypsin was removed from the 4°C refrigerator and warmed to room temperature prior to use. The large petri dish containing all of the Mn9D cells was

removed from the 37°C incubator and placed in a sterile hood. The cells and media were removed from the petri dish using an automatic pipette and discarded. The petri dish was washed once with 5mL PBS. The petri dish was gently tilted to ensure all areas of the petri dish had been washed and then the PBS was discarded using an automated pipette. Next, 1mL of trypsin was added to the petri dish and was sloshed gently over the cells. The petri dish was incubated in a 37°C incubator for 5 minutes. After incubation, 5mL of media was added to the petri dish and was gently washed over the cells. The cells and media were place into a falcon tube using an automated pipette. The tube was centrifuged at 1000 rpm for 5 minutes. After centrifuging, the supernatant was aspirated and discarded. Then, 1mL of warmed 10% FBS media was added to the tube and was gently swirled to disperse the cells in the media. Next, 9mL of additional media was added to the tube and the tube was gently pipetted up and down to break up clumps of cells. The cells and media were plated onto a new large petri dish and labeled in the format "Mn9D cells dd.mm.yy passage #."

After the cells had been cultured, the cells were counted to calculate the volume needed to plate 5,000 cells per well. First, the hemocytometer was cleaned using 70% isopropyl alcohol. Next, 10μL of the cell suspension was pipetted into one side of the hemocytometer. The hemocytometer was viewed under a microscope at 40x magnification. The cells were counted in each of the four counting squares and the concentrations in cells per mL were calculated as shown in Table 16.

Table 16. Calculations for Cell Counting

Calculation	Description
145 + 108 + 91 + 131 = 475	Added the number of cells counted in each of the four squares of the hemocytometer.
475 / 4 = 118.75 average	Divided the total number of cells by the total number of squares to calculate the average number of cells per square.
118.75 / 0.1 = 1,187.5	Divided the average number of cells by the 0.1 dilution.
1,187.5 (10,000) = 11,875,000 cells per mL	Multiplied by the volume of the hemocytometer to calculate the total cells per mL.

After calculating the concentration needed in cells per mL, more calculations were done to determine the volume needed to plate 5,000 cells per well as shown in Table 17.

Table 17. Calculations for 5,000 cells for a PDMS-coated 96 well plate

Calculation	Description
1 mL = 1000µL / 100µL = 10	To determine the concentration of cells per mL, one mL was divided by the volume of the plate.
5,000 cells per well (10 per mL) = 50,000 cells/mL	The number of cells desired per well was multiplied by the number of wells per mL to determine C_2
C_1 = 11,875,000/mL C_2 = 50,000 cells/mL 11,875,000 / 50,000 = 237.5x dilution	C_1 was divided by C_2 to determine the dilution needed.
Need 96 wells → Make enough for 100 wells 100 wells(100µL per well) = 10,000µL total volume	Calculated the total volume needed by multiplying the number of wells needed (plus a few extra just to be safe) by the volume of each well.
10,000µL total /237.5x = 42.1 µL ratio **Place 42.1 µL of C_1 in 9,957.9 µL media**	Divided the total volume by the dilution to determine the volume ratio. The volume ratio is the amount of C_1 to place in media, which has a volume of the total volume minus the volume ratio.

To dilute the total cell concentration to 5,000 cells in 100µL of media per well, 42.1µL of the initial cell concentration were placed in a falcon tube of 9,957.9µL of media. Then, 100µL of

the diluted solution was pipetted into each well of the PDMS-coated 96 well plate. The plate was labeled and placed in the 37°C incubator for four days to allow the spheroids to form. Cells were imaged using a 10x objective every day and about 25μL media was added to the wells every other day.

7.2 Validation

The project team validated the quality of the final design through several tests. First, by imaging the cells every day the team was able to assess the morphological changes during the formation of spheroids. Over the course of four days, the Mn9D cells spontaneously clumped together successfully forming spheroids. The project team used DAPI staining of cell nuceli to verify that the spheroids were actually composed of Mn9D cells. Next, the team assessed the compactness of the spheroids by calculating the sphericity of each spheroid that exhibited a high degree of compactness. The spheroids formed using the final design had the highest sphericity values of all of the design alternatives, thus verifying the quality of this design for 3D cell culture.

In addition to sphericity calculations, the project team used a confocal microscope to image the cell-to-cell interactions of the spheroids. The images verified the proximity of the cells to each other due to the 3D structure, which better models the cellular interactions of human tissue. Furthermore, the project team tested whether the spheroids were comparable to 2D cells by testing the spheroids' responsiveness to pesticides by using MTT assays. These MTT assays verified that the spheroids demonstrated the same trends of toxicity as the 2D Mn9D cells. All of the tests performed by the project team validated the functionality of the spheroids formed using the final design.

8.0 Conclusions and Future Recommendations

The project team successfully accomplished their goal of designing a repeatable, user friendly, and scalable cell suspension platform that facilitates three dimensional cell culture as an *in vitro* model to study the neurodegeneration caused by pesticides. The 96 well plate coated with PDMS met the team's first objective, reproducible, by forming spheroids with an average diameter of .958 ± .030 in four days. The second objective, user friendly, was also met because the design is comprised of standard laboratory equipment and requires very little preparation for use. Furthermore, the design is a modified 96 well plate, thus is compatible with any lab that already uses 96 well plates and is very intuitive to use. The third objective, scalable, was also met because 96 spheroids can be formed at one time using one PDMS-coated 96 well plate. This design is high throughput and efficient because it allows for the analysis of a large quantity of data without needed to transfer the cells to a different plate for analysis. Additionally, the design could be scaled up by using a 384 well plate rather than a 96 well plate, which enables researchers to screen many pesticides and analyze more toxicity data.

While there are many benefits of the project team's design, there are a few limitations. First, the PDMS-coated 96 well plate is not pre-made. The user must acquire the materials to make the PDMS coating and put it on the 96 well plate. Then, the user must sterilize the coated plate. This process, while relatively simple and quick, does require planning ahead and adds a small amount of extra time to the process of forming spheroids. Second, if the PDMS coating in the wells is too thick it can inhibit imaging. The wells must be carefully coated with PDMS to ensure that the whole bottom is covered, but there is not too much PDMS such that the wells cannot be imaged. Third, it is difficult to transfer the spheroids to a different plate because the spheroids can get stuck in the pipette tips. The project team tried to work around this limitation

by cutting the pipette tips to make a wider opening, but this technique did not completely eliminate the issue.

The project team suggests that future work on this design address the aforementioned limitations and the following recommendations. The first recommendation is to create a script in MATLAB or a similar program that can calculate sphericity automatically based on microscope images. This will greatly reduce the amount of time needed for analysis and will remove any bias from the results. The second recommendation is to experiment with different types of hydrophobic surface modifications for the formation of spheroids. The project team only had access to PDMS, but other potential designs could use a HEMA or an agarose coating. The third recommendation is to compare the Mn9D spheroids with spheroids formed from other cell types, such as HEK cells or human-derived neurons. The fourth recommendation is to do more research analyzing the functionality of the spheroids through calcium imaging. The project team attempted some preliminary calcium imaging, but had difficulties mounting the spheroids on the microscope stage used for calcium imaging, partially due to spheroids sticking to pipette tips. Because the project team had a short seven week time constraint, they could not perform pursue these recommendations. However, future work should pursue these recommendations to create an even better platform for facilitating three dimensional cell culture.

9.0 References

3D Biomatrix “Plate Handling and Spheroid Formation” (2013a) http://3dbiomatrix.com/wp-content/uploads/2013/10/Perfecta3D-HDP1096-Protocols_SF_Spheroid-Formation_05_13.pdf

3D Biomatrix. “Improving Compactness of Spheroids” (2013b) http://3dbiomatrix.com/wp-content/uploads/2013/10/Perfecta3D-Protocols_SF_Compactness-8_2013.pdf

Astashkina, A., Mann, B., Grainger, D.W. “A critical evaluation of in vitro cell culture models for high-throughput drug screening and toxicity.” *Pharmacology & Therapeutics*. 134 (2012): 82–106.

Betarbet, Ranjita, Todd Sherer, Gillian MacKenzie, Monica Garcia-Osuna, Alexander Panov, and Timothy Greenamyre. "Chronic Systemic Pesticide Exposure Reproduces Features of Parkinson's Disease." Nature Neuroscience 3 (2000): 1301-306. Print.

Brown, R. C., Lockwood, A. H., & Sonawane, B. R. (2005). Neurodegenerative Diseases: Environmental Risk Factors – An Overview. *Environmental Health Perspectives*, *113*(9), 1250–1256.

Cannon, J. R., & Greenamyre, J. T. (2011). The role of environmental exposures in neurodegeneration and neurodegenerative diseases. *Toxicological Sciences*,*124*(2), 225-250.

Casquillas, Guilhem V. "PDMS: A Review." *Microfluidic Innovation Center*. Elveflow, 2013. Web. 15 Nov. 2013.

Chan, C. S., Gertler, T. S., & Surmeier, D. J. (2009). Calcium homeostasis, selective vulnerability and Parkinson's disease. *Trends in neurosciences*, *32*(5), 249-256.

Dow Corning. “Physical and chemical properties of silicone (polydimethylsiloxane): A unique semi-organic structure.” 2012. Web.

Drolet, R. E., Cannon, J. R., Montero, L., & Greenamyre, J. T. (2009). Chronic rotenone exposure reproduces Parkinson's disease gastrointestinal neuropathology. *Neurobiology of disease*, *36*(1), 96-102.

Fan S.F., Shen K.F., Scheideler M.A., and Crain S.M. “F11 neuroblastoma x DRG neuron hybrid cells express inhibitory mu- and delta-opioid receptors which increase voltage-dependent K+ currents upon activation.” *Brain Res* 590 (1992) 329-333.

Fendinger, N. J. (2000). Polydimethylsiloxane (PDMS): Environmental Fate and Effects. *Organosilicon Chemistry Set: From Molecules to Materials*, 626-638. Web.

Franco, Rodrigo, Sumin Li, Humberto Rodriguez-Rocha, Michaela Burns, and Mihalis I. Panayiotidis. "Molecular Mechanisms of Pesticide-induced Neurotoxicity: Relevance to Parkinson's Disease." *Chemico-Biological Interactions* 188.2 (2010): 289-300.

Fraley S.I., Feng Y., Krishnamurthy R., Kim D.H., Celedon A., Longmore G.D., Wirtz D. "A distinctive role for focal adhesion proteins in three-dimensional cell motility." *Nat Cell Biol* 12(2010) 598-604.

Freestone PS, Chung KKH, Guatteo E, Mercuri NB, Nicholson LFB, Lipski J. Acute action of rotenone on nigral dopaminergic neurons involvement of reactive oxygen species and disruption of Ca^{2+} homeostasis. *Eur. J. Neurosci*. 30: 1849–1859, 2009.

Friedrich, J., Seidel, C., Ebner, R., & Kunz-Schughart, L. A. (2009). Spheroid-based drug screen: considerations and practical approach. *Nature protocols*,*4*(3), 309-324.

Garbarini N. "Primates as a model for research." *Disease Models & Mechanisms* 3 (2010): 15-19.

Ghosh S., Spagnoli G.C., Martin I., Ploegert S., Demougin P., Heberer M., Reschner A. "Three-dimensional culture of melanoma cells profoundly affects gene expression profile: a high density oligonucleotide array study." *J Cell Physiol* 204(2005): 522-531.

Goulson, D. "Neonicotinoids and Bees." Significance 10.3 (2013): 6-11. Print.

Grosset, D., Fernandez, H., & Okun, M. (2009). *Parkinson's Disease: Clinican's Desk Reference*. Manson Publishing.

Hatcher, J. M., Pennell, K. D., & Miller, G. W. (2008). Parkinson's disease and pesticides: a toxicological perspective. *Trends in pharmacological sciences*,*29*(6), 322-329.

Hisahara, S., & Shimohama, S. (2011). Dopamine Receptors and Parkinson's Disease. International Journal of Medicinal Chemistry, 2011.

Huh, D., Hamilton, G.A., & Ingber, D.E. "From 3D Cell Culture to Organs-on-chips." *Trends in Cell Biology* 21.12 (2011): 745-754.

Hwang, O. (2013). Role of Oxidative Stress in Parkinson's Disease. *Experimental neurobiology*, *22*(1), 11-17.

"Imidacloprid Technical Fact Sheet." National Pesticide Information Center. Oregon State University, n.d. Web. 11 Nov. 2013.

"International Code of Conduct on the Distribution and Use of Pesticides." FAO Corporate Document Repository. Agriculture and Consumer Protection, 2003. Web. 14 Oct. 2013.

Ivascu, A., & Kubbies, M. (2006). Rapid generation of single-tumor spheroids for high-throughput cell function and toxicity analysis. *Journal of biomolecular screening*, *11*(8), 922-932.

Janda, Elzbieta, Ciro Isidoro, Cristina Carresi, and Vincenzo Mollace. "Defective Autophagy in Parkinson's Disease: Role of Oxidative Stress." *Molecular Neurobiology* 46.3 (2012): 639-61. *Springer Link.*

Jenner, P. (2003). Oxidative stress in Parkinson's disease. *Annals of neurology*,*53*(S3), S26-S38.

Kang H., Han B., Kim S. "Mechanisms to prevent caspase activation in rotenone-induced dopaminergic neurodegeneration: role of ATP depletion and procaspase-9 degradation." *Apoptosis* 17 (2012):449–462

Kim, Yonjung, Myoung Kyu Park, Dae-Yong Uhm, and Sungkwon Chung. "Modulation of T-type Ca2 Channels by Corticotropin-releasing Factor through Protein Kinase C Pathway in MN9D Dopaminergic Cells." *Biochemical and Biophysical Research Communications* 358.3 (2007): 796-801.

Kimura-Kuroda, Junko, Yukari Komuta, Yoichiro Kuroda, Masaharu Hayashi, and Hitoshi Kawan. "Nicotine-Like Effects of the Neonicotinoid Insecticides Acetamiprid and Imidacloprid on Cerebellar Neurons from Neonatal Rats." PLOS One 7.2 (2012): n. pag. Print.

Laycock, Ian, Kate Lenthall, Andrew Barratt, and James E. Cresswell. "Effects of Imidacloprid, a Neonicotinoid Pesticide, on Reproduction in Worker Bumble Bees." Ecotoxicology (2012): n. pag. Print.

Le Couteur, D. G., McLean, A. J., Taylor, M. C., Woodham, B. L., & Board, P. G. (1999). Pesticides and Parkinson's disease. *Biomedicine & pharmacotherapy*, *53*(3), 122-130.

Lee, W. G., Ortmann, D., Hancock, M. J., Bae, H., & Khademhosseini, A. (2009). A hollow sphere soft lithography approach for long-term hanging drop methods. *Tissue Engineering Part C: Methods*, *16*(2), 249-259. Web.

"Lethal Dosage (LD50) Values." *EPA*. Environmental Protection Agency, 27 June 2012. Web. 14 Oct. 2013.

Legradi A., Varszegi S., Szigeti C., Gulya K. "Adult rat hippocampal slices as *in vitro* models for neurodegeneration: Studies on cell viability and apoptotic processes." *Brain Res Bull*. 84 (2011): 39-44.

Lotharius, J., & Brundin, P. (2002). Pathogenesis of Parkinson's disease: dopamine, vesicles and α-synuclein. Nature Reviews Neuroscience, 3(12), 932-942.

Mangano E.N., Litteljohn D., So R., Nelson E., Peters S., Bethune C., Bobyn J., Hayley S., "Interferon-γ plays a role in paraquat-induced neurodegeneration involving oxidative and proinflammatory pathways." *Neurobiology of Aging* 33:7 (2012): 1411-1426.

Mann, CJ. "Observational and Research Methods. Research Design II: Cohort, Cross Sectional, and Case Control Studies." Emerg Med J 20 (2003): 54-60.

Manning-Bog, A. B., McCormack, A. L., Li, J., Uversky, V. N., Fink, A. L., & Di Monte, D. A. (2002). The Herbicide Paraquat Causes Up-regulation and Aggregation of α-Synuclein in Mice PARAQUAT AND α-SYNUCLEIN. Journal of Biological Chemistry, 277(3), 1641-1644.

Malev O., Sauerborn Klobučar R., Fabbretti E., Trebše P. (2012) Comparative toxicity of imidacloprid and its transformation product 6-chloronicotinic acid to non-target aquatic organisms : microalgae Desmodesmus subspicatus and amphipod Gammarus fossarum. *Pesticide Biochemistry and Physiology*. 32.

Marambaud, P., Dreses-Werringloer, U., & Vingtdeux, V. (2009). Calcium signaling in neurodegeneration. Mol Neurodegener, 4(20), 6-5.

Marella M, Seo BB, Nakamaru-Ogiso E, Greenamyre JT, Matsuno-Yagi A. "Protection by the NDI1 Gene against Neurodegeneration in a Rotenone Rat Model of Parkinson's Disease." PLoS ONE 3(1) (2008): e1433

"Microtissues." *Microtissues Natural 3D*. Sigma-Aldrich, 2013. Web. 15 Nov. 2013

Mostafalou, Sara, and Mohammad Abdollahi. "Pesticides and Human Chronic Diseases: Evidences, Mechanisms, and Perspectives." Toxicology and Applied Pharmacology 268.2 (2013): 157-77. Print.

Obeso, J. A., Rodriguez-Oroz, M. C., Goetz, C. G., Marin, C., Kordower, J. H., Rodriguez, M.& Halliday, G. (2010). Missing pieces in the Parkinson's disease puzzle. Nature medicine, 16(6), 653-661.

Osborne, J. L. (2012). Ecology: Bumblebees and pesticides. *Nature*, *491*(7422), 43-45.

Pampaloni, F., Ansari, N., Stelzer, E.H.K. "High-resolution deep imaging of live cellular spheroids with light-sheet-based fluorescence microscopy." *Cell Tissue Res.* 352(2013) 161-177.

Panov, Alexander, Sergey Dikalov, Natalia Shalbuyeva, Georgia Taylor, Todd Sherer, and TImothy J. Greenamyre. "Rotenone Model of Parkinson Disease: Multiple Brain Mitochondria Dysfunctions After Short Term Systemic Rotenone Intoxication." Journal of Biological Chemistry 280.51 (2005): 42026-2035.

"Protocols." *3D Biomatrix*. 3D Biomatrix, 2013. Web. 15 Nov. 2013

"Reproducible and Uniform Embryoid Bodies Using AggreWell Plates." STEMCELL Technologies, 2013. Web. 15 Nov. 2013.

Ratnayaka, S. H., Hillburn, T. E., Forouzan, O., Shevkoplyas, S. S., & Khismatullin, D. B. (2013). PDMS well platform for culturing millimeter-size tumor spheroids. *Biotechnology progress*. Web.

Rimann, M., and Graf-Hausner, U. "Synthetic 3D Multicellular Systems for Drug Development." *Current Opinion in Biotechnology* 23 (2012): 803-809.

Sánchez-Pérez, A. M., Claramonte-Clausell, B., Sánchez-Andrés, J. V., & Herrero, M. T. (2012). Parkinson's disease and autophagy. Parkinson's disease, 2012.

Sherer, Todd B., Ranjita Betarbet, Claudia M. Testa, Byoung Boo Seo, Jason R. Richardson, and Jin Ho Kim. "Mechanism of Toxicity in Rotenone Models of Parkinson's Disease." The Journal of Neuroscience 23.34 (2003): 10756-0764. Print.

Surmeier, D. J. (2007). Calcium, ageing, and neuronal vulnerability in Parkinson's disease. *The Lancet Neurology*, *6*(10), 933-938.

Talbot, Janet, Gavriel David, Ellen Barrett, and John Barrett. "Calcium Dependence of Damage to Mouse Motor Nerve Terminals following Oxygen/ Glucose Deprivation." *Experimental Neurology* 234 (2012): 95-104.

Tapias V., Cannon J.R., and Greenamyre J.T. "Melatonin Treatment Potentiates Neurodegeneration in a Rat Rotenone Parkinson's Disease Model." *Journal of Neuroscience Research* 88 (2010): 420–427.

Thiffault, C., Langston, J. W., & Di Monte, D. A. (2000). Increased striatal dopamine turnover following acute administration of rotenone to mice. Brain research, 885(2), 283-288.

Radad, K., G. Gille, and W. Rausch. "Dopaminergic Neurons Are Preferentially Sensitive to Long-term Rotenone Toxicity in Primary Cell Culture." *Toxicology in Vitro* 22.1 (2008): 68-74.

Zhou, C., Huang, Y., & Przedborski, S. (2008). Oxidative stress in Parkinson's disease. *Annals of the New York Academy of Sciences*, *1147*(1), 93-104.

Van Der Mark, Marianne, Maartje Brouwer, Hans Kromhout, Peter Nijssen, Anke Huss, and Roel Vermeulen. "Is Pesticide Use Related to Parkinson's Disease? Some Clues to Heterogeneity in Study Results." Environmental Health Perspectives 120.3 (2011): 340-47. Print.

Visan, Anke, Katrin Hayess, Dana Sittner, Elena Pohl, Christian Riebeling, Birgitta Slawik, Konrad Gulich, Michael Oelgeschlager, Andreas Luch, and Andrea Seiler. "Neural Differentiation of Mouse Embryonic Stem Cells as a Tool to Assess Developmental Neurotoxicity *in vitro*." *NeuroToxicology* 33 (2012): 1135-146.

Whitesides, G. M. (2006). The origins and the future of microfluidics. *Nature*,*442*(7101), 368-373.

10.0 Appendices

Appendix A: Objectives Tree

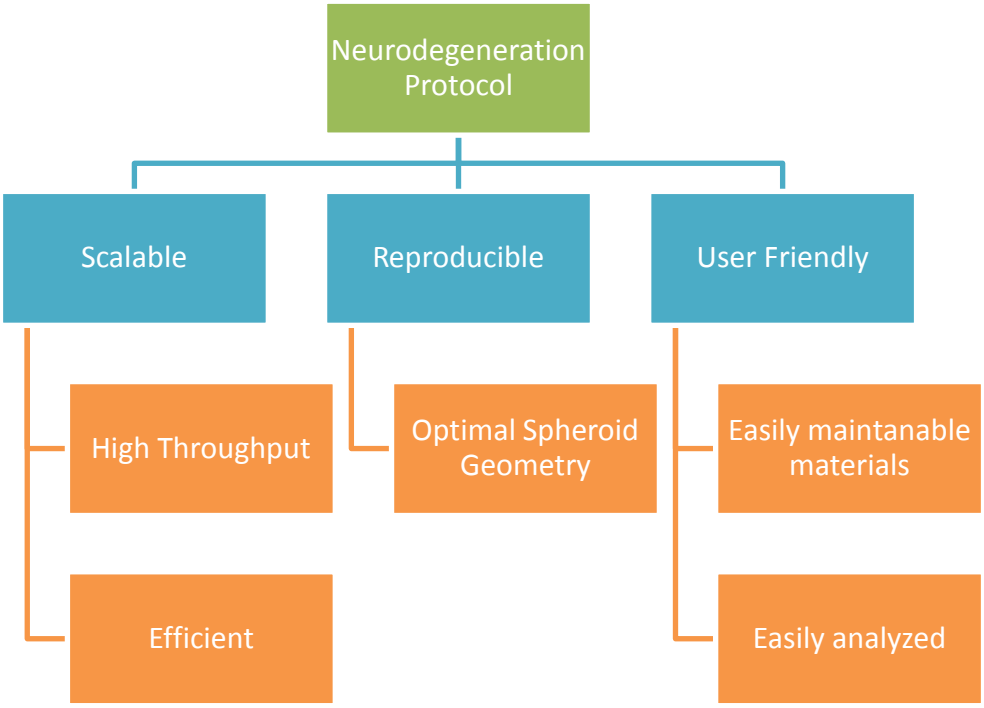

Appendix B: Pairwise Comparison Chart

Objectives	Scalable	Reproducible	User Friendly	Score
Scalable	--	0	0	0
Reproducible	1	--	1	2
User Friendly	1	0	--	1

Appendix C: Gantt Chart

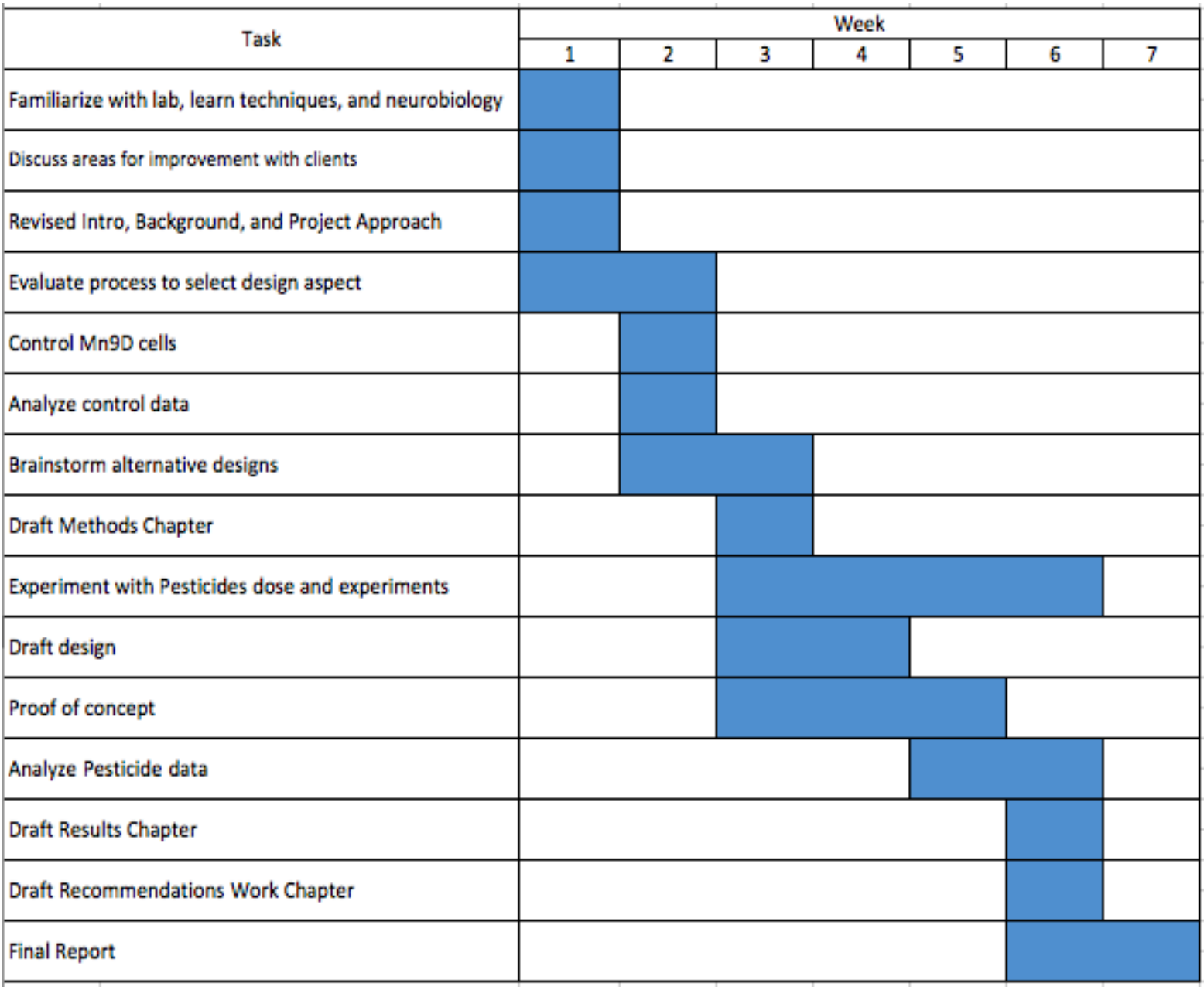

Appendix D: Work Breakdown Structure

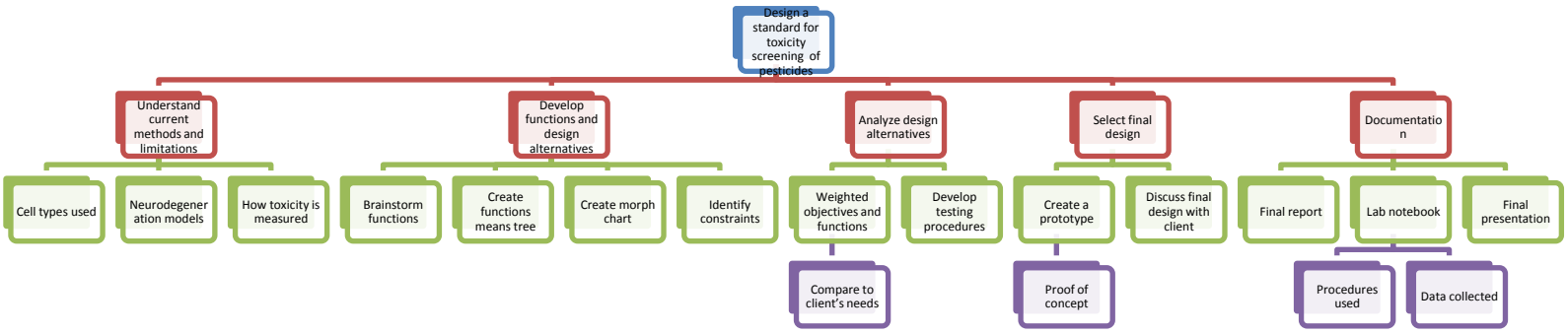

Appendix E: Plating 2D 96-Well Plates

1. Placed 50 µL of polylysine in each well
    a. Polylysine → stock 1mg/mL → 40µL in 1 mL of water
        i. 50µL per well = 2.4 mL total needed
        ii. 120 µL of polylysine placed in 3 mL of water
2. 50 µL of polylysine solution was placed in each well.
3. The plate then sat for 20 minutes.
4. Polylysine was then aspirated from the wells using a vacuum and wasted.
5. The wells were then washed 3x with DI water.
6. The plate was left to dry completely.
7. Cells were counted and split using the cell culture protocol and the cells were diluted to the correct concentration as shown in section 4.5.1.
8. Doxycycline was added to this concentration using a 1µL to 1mL ratio.
9. 100µL of the concentration was added to each well of the 96-well plate.
10. Once the cell suspension has been plated, the plate was covered and placed in the incubator for 4 days to form spheroids.
11. The plate was imaged each day to document progress.

Appendix F: Plating 3D Drops on Petri Dishes

1. Cells were counted and split using the cell culture protocol and the cells were diluted to the correct concentration as shown in section 4.5.1.
2. Doxycycline was added to this concentration using a 1µL to 1mL ratio.
3. 4 - 40µL drops of the concentration were placed on the inside of the top of the Petri Dish.
4. Once the cell suspension has been plated, the top of the petri dish was flipped carefully as the drops hung from the top of the dish.
5. 2 mL of PBS was added to the bottom of the petri dish to keep the hanging drops from drying out.
6. The plate was then covered and placed in the incubator for 4 days to form spheroids.
7. The plates were imaged each day to document progress.

Appendix G: Plating Hanging Drop Plate

1. Cells were counted and split using the cell culture protocol and the cells were diluted to the correct concentration as shown in section 4.5.1.
2. Doxycycline was added to this concentration using a 1µL to 1mL ratio.
3. 2mL of DI water was added to the plate reservoir and 1mL of DI water was added to the tray reservoirs prior to plating cells.
4. Once the DI water has been added to the reservoirs and the plate has been assembled, plating can begin.
5. 40µL of the cell suspension was added to each well of the 96 well hanging drop plate.
6. To pipet the cell suspension into the well plate, the pipet tip must be at least halfway into the well without coming in contact with the tray.
7. Once the hanging drops have been created, the plate was covered and placed in the incubator for 4 days to form spheroids.
8. The plate was imaged each day to document progress.

Appendix H: Plating Shrinky Dinks

**borrowed from: Shrinky-Dink Hanging Drops: A Simple Way to Form and Culture Embryoid Bodies – Chi-Shuo Chen, Jonathan Pegan and Michelle Khine

1. Making the Shrinky-Dink Mold
    a. Print the desired pattern on shrink-dink paper using a printer
        i. Note: Run through printer twice if mold doesn't work the first time
    b. Bake shrinky-dink sheet at 163° C for about 10 minutes, or until fully shrunk
    c. Submerge it in an isopropanol bath until the complete surface is barely covered.
    d. Carefully, spray some acetone over the mold and shake container a few times. Add more isopropanol to wash out acetone excess and repeat this step a few times until shrinky-mold looks clean.
    e. Immerse mold in distilled water for 10 mins to wash off remaining organic solvent.
    f. Air clean shrinky-mold. Re-heat it for about 5 minutes at 163° C. This will compact ink and evaporate any remaining solvent.
2. Making PDMS microwells
    a. Prepare a 10:1 PDMS/curing agent mixture, and agitate vigorously for few minutes.
    b. Place shrink-dink mold in a small petri dish. Pour PDMS mixture until it reaches about ½ cm over the mold surface.
    c. Let sit until most air bubbles are out
    d. Cut off PDMS from mold and bind it to a glass slide just by applying pressure.
    e. Discard first microwell-chip, since it has ink residues incrusted between PDMS.
    f. Repeat this procedure to produce a second chip that is ink-free and has a more defined shape.
    g. Clean microwell-chip using 70% ethanol solution. Place it under UV light source for 10 minutes to sterilize it.
3. Trapping cells in microwells
    a. Count cells and dilute them in culture media to desired concentration. For example to get 10-15 cells per well use a concentration of 8×10^4 cells/ml,
    b. Carefully place microwell chip in a 50 ml centrifuge tube containing solidified PDMS base.
    c. Add about 2 ml of cell solution.
    d. Centrifuge for 5 minutes at 760 rpm and 4 °C.
    e. Pipet out excess solution and carefully wash microwell with PBS 1X solution.
    f. Place microwell in a small petry dish, being careful while taking the chip out of the centrifuge tube.
    g. Wash cell excess using 1 X PBS solution.
    h. Place microwell chip under an inverted microscope to verify intended number of cells/well.
    i. Incubate microwell containing cells at standard conditions.

Appendix I: Creating PDMS Coated Petri Dishes

1. PDMS was created using a 10:1 ratio of silicone elastomer (10) and silicone elastomer curing agent (1).
2. The two ingredients were stirred until there were no bubbles present.
3. Approximately 1000µL of PDMS was pipetted into each cover of the petri dishes.
4. Once they were filled, the petri dishes were placed in the oven at 80°C for about 20 minutes to solidify before use.
5. Once the PDMS was solidified, they were covered with ethanol and placed in a sterile hood and exposed to UV light for a half hour to be sterilized.
6. They were then aspirated of ethanol and washed 3x with PBS before being used to plate Mn9D cells.

Appendix J: Creating PDMS-coated 24 well plates

1. PDMS was created using a 10:1 ratio of silicone elastomer (10) and silicone elastomer curing agent (1).
2. The two ingredients were stirred until there were no bubbles present.
3. Approximately 200µL of PDMS was pipetted into each well of the 24well plate.
4. Once they were filled, the 24 well plate was placed in the oven at 80°C for about 20 minutes to solidify before use.
5. Once the PDMS was solidified, they were covered with ethanol and placed in a sterile hood and exposed to UV light for a half hour to be sterilized.
6. They were then aspirated of ethanol and washed 3x with PBS before being used to plate Mn9D cells.

Appendix K: Creating PDMS-coated 96 well plates

7. PDMS was created using a 10:1 ratio of silicone elastomer (10) and silicone elastomer curing agent (1).
8. The two ingredients were stirred until there were no bubbles present.
9. Approximately 100µL of PDMS was pipetted into each well of the 96-well plate.
10. Once they were filled, the 96-well plate was placed in the oven at 80°C for about 20 minutes to solidify before use.
11. Once the PDMS was solidified, they were covered with ethanol and placed in a sterile hood and exposed to UV light for a half hour to be sterilized.
12. They were then aspirated of ethanol and washed 3x with PBS before being used to plate Mn9D cells.

Appendix L: Creating Agarose-coated 24 well plates and 96 well plates

Preparing the Agarose Coated Plates:

1. Create the solution of agarose
    a. Add 1g of agarose to 100 mL of deionized water (1%) –(**Human Neuroendocrine Tumor Cell Lines as Three-Dimensional Model for the Study of Human Neuroendocrine Tumor Therapy**)
        i. 1% agarose solution was made with agarose G-10 and dieionized water and heated until boiling in microwave (**The effect of forced growth of cells into 3D spheres using low attachment surfaces on the acquisition of stemness properties)**
        ii. Equal volumes of pre-warmed DMEM medium and 1% agarose solution was mixed for coating. (**The effect of forced growth of cells into 3D spheres using low attachment surfaces on the acquisition of stemness properties**)
        iii. OR - .15 g agarose to 10 mL of DMEM (1.5 wt%/vol) (**spheroid based drug screen: considerations and practical approach)**
2. Autoclave and sterilize in a 250 mL – 500 mL bottle (**Human Neuroendocrine Tumor Cell Lines as Three-Dimensional Model for the Study of Human Neuroendocrine Tumor Therapy)**
    a. Autoclave for 20 min at 120˚C, 2 bar (**spheroid based drug screen: considerations and practical approach)-** open oven at 90 ˚C
        i. ** note don't allow agarose to cool and solidify
3. Transfer bottle into 60 – 70 ˚C water bath for 1 hour(**Human Neuroendocrine Tumor Cell Lines as Three-Dimensional Model for the Study of Human Neuroendocrine Tumor Therapy)**
4. Pipette agarose into each well
    a. 50 µL for a 96 well plate (**spheroid based drug screen: considerations and practical approach)**
    b. 200 µL for 24 well plate (**Human Neuroendocrine Tumor Cell Lines as Three-Dimensional Model for the Study of Human Neuroendocrine Tumor Therapy)**
5. Coated plate should be ready to use in seconds to minutes (10 - 20 minutes according to – want to allow the plate to cool down - **Human Neuroendocrine Tumor Cell Lines as Three-Dimensional Model for the Study of Human Neuroendocrine Tumor Therapy)**
    a. They can be stored at room temperature away from light for up to 10 days

Adding Cell Suspension to Agarose Coated Plates:

1. Using a 24 well plate to get 400 µm spheroids(human neuroendocrine tumor cell lines) – (**Human Neuroendocrine Tumor Cell Lines as Three-Dimensional Model for the Study of Human Neuroendocrine Tumor Therapy)**
    a. Dispensed 1,000 cells/ 200 µL in each well ** can look up if maybe there's a better concentration that can be used
    b. Sealed the well plate with sterile sealing tape (parafilm would probably work)
    c. Overnight the cells were placed on a oribital shaker and incubated overnight
    d. Next day move the well-plate off the shaker and continue to incubate
    e. Every 3 days add 200 µL of growth medium (will do twice)
    f. Should be grown after 6 days
2. Using a 96 well plate to get 400 µm spheroids (**spheroid based drug screen: considerations and practical approach)**
    a. Dispense 200 µL of cell suspension in each well
        i. They used: 7500 cells/mL for HT29 cells and 3,500 cells/mL for HCT-116 cells – both human carcinoma cells
        ii. The plates were then incubated for 4 days avoiding agitation (they did not change or add any medium)

Appendix M: 3D Mold CAD Drawings

Sleeve Covering Base

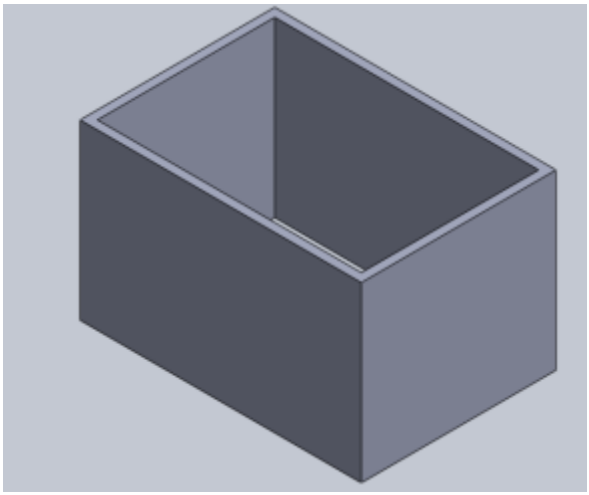

Round Well

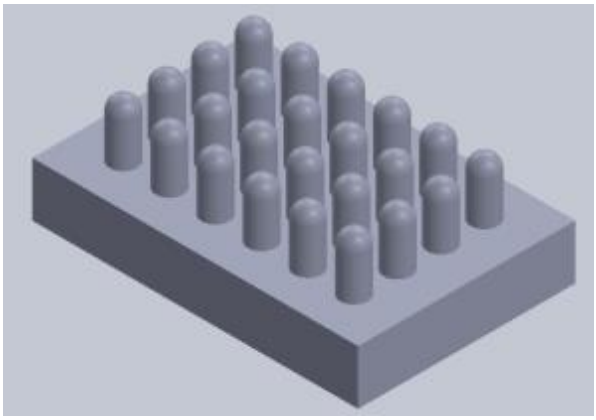

Truncated Cone Well

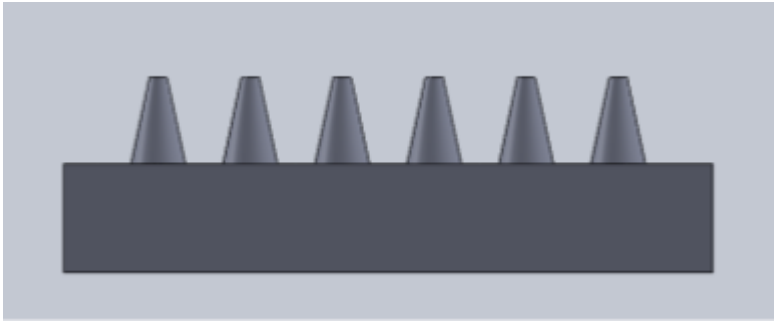

Pyramid Well

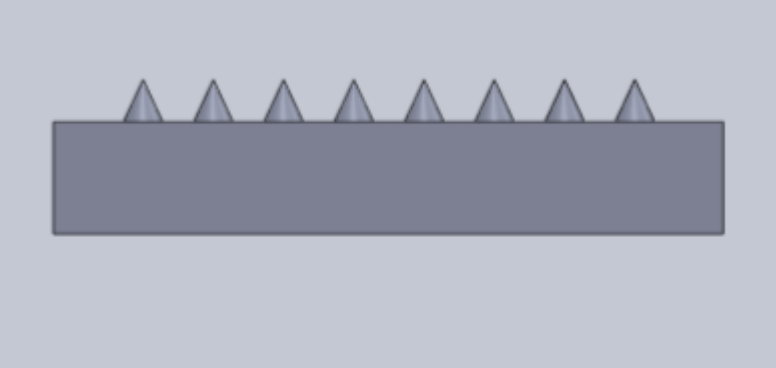

Rod-Well Cone

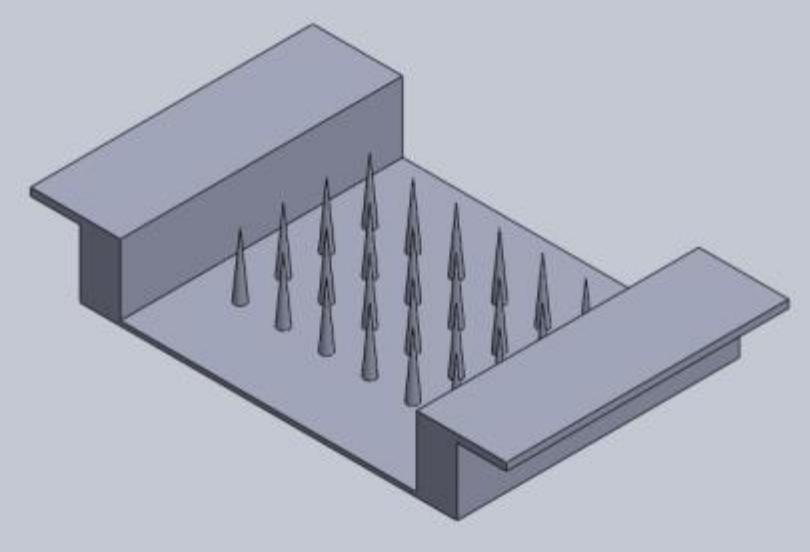

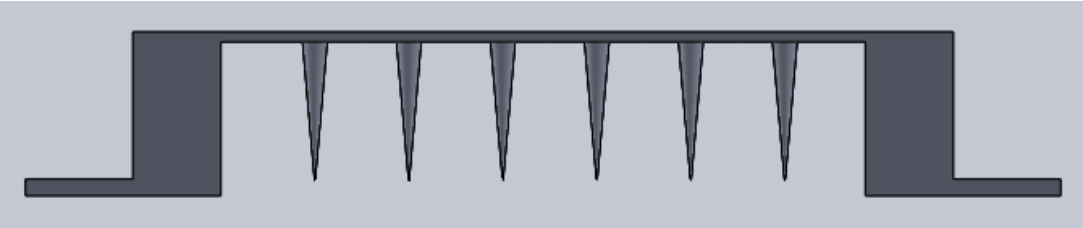

Rod-Well Round

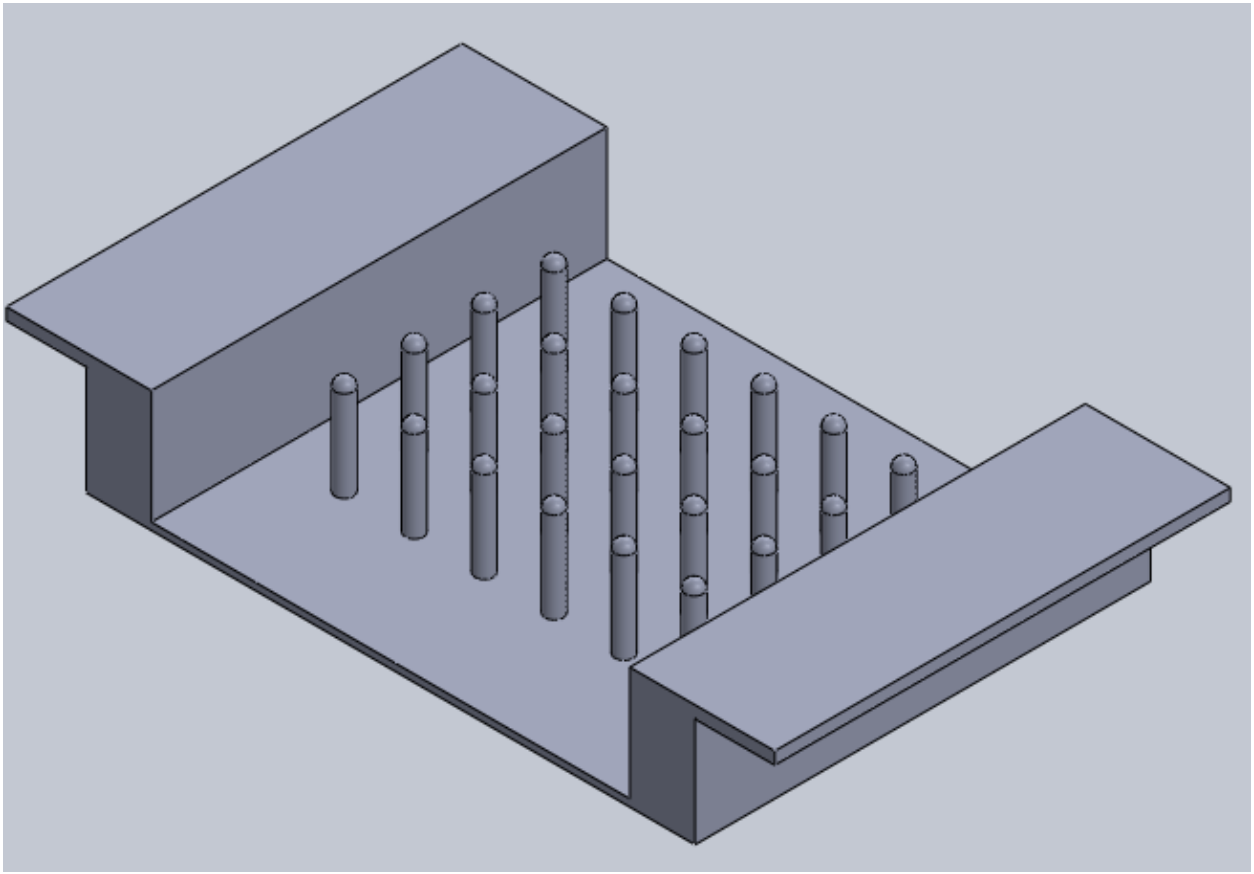

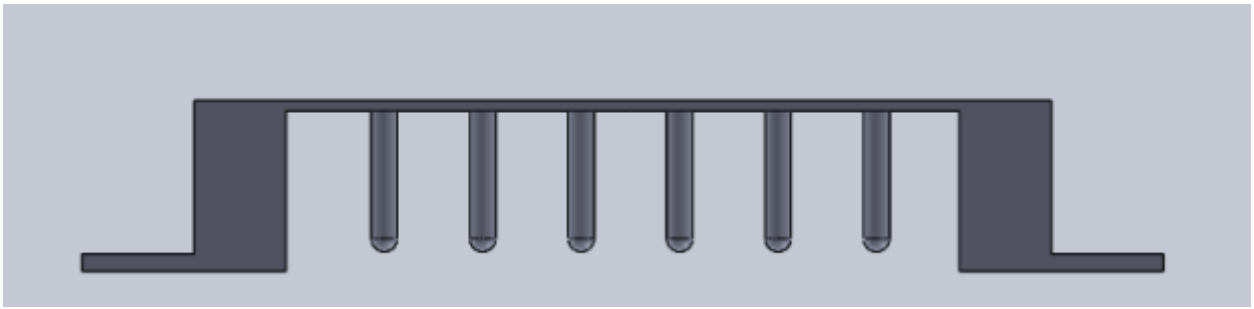

Appendix N: Creating PDMS Molds

1. PDMS was created using a 10:1 ratio of silicone elastomer (10) and silicone elastomer curing agent (1).
2. The two ingredients were stirred until there were no bubbles present.
3. Approximately 28 grams of PDMS was used to fill the 3D printed molds.
4. Once they were filled, the molds were left to sit over the weekend to solidify.
5. On Monday, the molds were extruded from the 3D platforms and baked in the oven for an hour at 80°C to finish casting.
6. Once the molds were solidified, they were covered with ethanol and placed in a sterile hood and exposed to UV light for a half hour to be sterilized.
7. They were then aspirated of ethanol and washed 3x with PBS before being used to plate Mn9D cells.

Appendix O: Creating 10% FBS Media for Mn9D Cells

1. The components needed were calculated to make a 200mL total final volume of media with 10% FBS in it.
    a. 100 mL DMEM(1X) + GutaMax
    b. 90 mL F-12 Nut Mix (1x) + GlutaMax + Pen/Strep
    c. 10 mL FBS
2. 100 mL of DMEM and 90 mL of F-12 was then mixed together.
3. The FBS was filtered to prevent contamination.
    a. 5mL of FBS was placed in 0.45µm filter into falcon tube.
    b. Plunger was used to force FBS through the filter.
    c. This was repeated for an additional 5 mL of FBS.
4. 10 mL of filtered FBS was added to the DMEM + F-12 solution.
5. The media was then placed in the water bath to warm until needed.

Appendix P: Cell Culturing of Mn9D Cells

1. Remove Trypsin from the fridge and warmed to room temperature.
2. Remove Mn9D media from the fridge and place it in the water bath.
3. Remove the cells from the petri dish and place in a falcon tube.
4. Wash the cells on the petri dish 1 time with 5 mL of PBS, gently over the cells and discard PBS when washed.
5. Add 1 mL of trypsin and slosh gently over the cells.
6. Incubate cells at 37°C for 5 minutes.
7. View cells under a microscope.
8. 5 mL of media was added to the petri dish and run over the cells.
9. The media was removed and collected in a separate falcon tube.
10. The tubes were both centrifuged for 5 minutes.
11. The supernatant of both tubes was aspirated and discarded.
12. 1mL of 10% FBS media was added to the tube and gently swirled and both tubes were combined into one.
13. 9 more mL of media was added to the tube.
14. The media was pipetted up and down multiple times to break up clumps of cells.
15. Cells were then replated onto a petri dish and labeled with the name of the cells, date and the passage number.

Appendix Q: DAPI Staining

1. Aspirate wells desired for DAPI stain.
2. Mix 1000µL of PBS and 1 µL of DAPI stain in an eppendorf tube.
3. Add enough DAPI stain solution to cover the bottom of each well.
4. Let the DAPI stain sit on cells for 5 minutes.
5. Aspirate stain and add 100µL of PBS to each well.

Appendix R: MTT Assay

1. 50 mg of MTT Assay powder was weighed our and dissolved in 20mL of phenol free medium.
2. For 2D, calculated enough solution for 100µL total volume per well for 24 wells, giving us 3mL total of MTT solution and media.
3. With a 5x concentration, a total of 600µL of MTT solution was diluted in 2.4mL of media, giving us a total of 20 µL of MTT solution per well.
4. Before plating the MTT solution in the well, the wells were first aspirated of media/pesticide solution and discarded.
5. Then 100µL of the final MTT/Media solution was added to each well.
6. The plate was then placed in the incubator for 2 hours.
7. After 2 hours, the plate was retrieved from the incubator and the MTT solution was aspirated.
8. 100µL of DMSO was added to each well.
9. The plate was then wrapped in aluminum foil and transferred to COBIK in Ajdovina for analysis.
10. The plate was analyzed at 570 nm and subtracted 670 nm.

Appendix S: Results

Average Sphericity Score on Day 4

Rank	Non-coated Petri-Dish	PDMS Coated Petri-Dish	PDMS Coated 96 Well Plate	Perfecta 3D Hanging Drop Kit	Non-Coated 96 Well Plate (Control)
1	0	12	20	10	0
2	2	4	18	19	0
3	2	8	2	24	0
4	0	4	0	11	0
5	0	4	1	0	96
6	4	28	7	32	0
Total Plated	8	60	48	96	96
Average Score	**4.25**	**4.13**	**2.27**	**3.71**	**5**

Average Sphericity Score on Day 7

Rank	Non-coated Petri-Dish	PDMS Coated Petri-Dish	PDMS Coated 96 Well Plate	Perfecta 3D Hanging Drop Kit	Non-Coated 96 Well Plate (Control)
1	0	18	10	10	0
2	3	8	10	11	0
3	1	4	18	32	0
4	0	0	0	0	0
5	0	1	0	0	96
6	4	29	10	43	0
Total Plated	8	60	48	96	96
Average Score	**4.25**	**3.75**	**3.00**	**3.48**	**5**

Average Spheroid Diameter

Device	Day	Cells Averaged	Average Cell Diameter (µm)
Non-Coated Petri Dish	4	2	265
	7	3	203
PDMS Coated Petri Dish	4	16	396
	7	26	394
PDMS Coated 96 Well Plate	4	38	302
	7	20	356
Perfecta 3D Hanging Drop	4	29	424
	7	21	593
Agarose Coated 24-well plate	4	Dried Up	N/A
	7	Dried Up	N/A
Shrinky-dinks	4	Couldn't find cells	N/A
	7	Couldn't find cells	N/A
3D Printed Molds	4	Couldn't find cells	N/A
	7	Couldn't find cells	N/A

Average Spheroicity

Device	Day	Cells Averaged	Average Cell Sphericity
Non-Coated Petri Dish	4	2	.963
	7	3	.968
PDMS Coated Petri Dish	4	16	.963
	7	26	.982
PDMS Coated 96 Well Plate	4	38	.970
	7	20	.967
Perfecta 3D Hanging Drop	4	29	.958
	7	21	.952

Appendix T: Abbreviations

PD = Parkinson's Disease

FBS = Fetal Bovine Serum

Ca^{2+} = Calcium

2D = Two-dimensional

3D = Three-dimensional

ROS = Reactive oxygen species

FAO = Food and Agriculture Organisation

IMI = Imidacloprid

PBS = Phosphate Buffered Saline

ABS = Acrylonitrile butadiene styrene

PLA = Polylactic acid

PET = Polyethylene terephthalate

MTT = Microculture Tetrazolium